Magnetoforeza w zawiesinach magnetycznych

Maciej Urbaniak
IFM PAN 2010.10.15

Magnetophoresis in magnetic suspensions

1. Forces in magnetic field
2. Microseparation
3. Controlled propulsion
4. Use of secondary flow

Resources:

[1] Martin A. M. Gijs, Frédéric Lacharme, and Ulrike Lehmann, Chamical Reviews **110**, 1518 (2010)

[2] Chiun-Peng Lee and Mei_Feng Lai, J. Appl. Phys. **107**, 09B524 (2010)

[3] Hisao Morimoto et al., Phys. Rev. E **78**, 021403 (2008)

[4] Pietro Tierno, Thomas M. Fischer, Tom H. Johansen, and Francesc Saguès, Phys. Rev. Lett. **100**, 148304 (2008)

[5] Pietro Tierno, Sathavaram V. Reddy, Jing Yuan, Tom H. Johansen, and Thomas M. Fischer, J. Phys. Chem. B , **111**, 13479 (2007)

[6] Alejandro Soba, Pietro Tierno, Thomas M. Fischer, and Francesc Saguès, Physical Review E **77**, 060401R (2008)

[7] Charles E. Sing, Lothar Schmid, Matthias F. Schneider, Thomas Franke, and Alfredo Alexander-Katz, Proceedings of the National Academy of Sciences of the United States of America, **107**, 535 (2010)

[8] Tanja Weis, *Fernsteuerung superparamagnetischer Partikel und Charakterisierung von Magnetkraftmikroskopiespitzen in externen Magnetfeldern mit magnetisch strukturierten Substraten*, Kassel 2009

[9] Miltenyi_Biotec_Catalog2009.pdf, www.miltenyibiotec.com

[10] C. S. Lee, H. Lee, and R. M. Westervelt, Appl. Phys. Lett. **79**, 3308 (2001)

[11] I. Šafařik, M. Šafařıková, Journal of Chromatography B, **722**, 33–53 (1999)

[12] Q. A. Pankhurst, J. Connolly, S. K. Jones, J. Dobson, J. Phys. D: Appl. Phys., **36**, R167 (2003)

[13] www.wikipedia.org

[14] P.W. Kuchel, B.E. Chapman, W.A. Bubb, P.E. Hansen, C.J. Durrant,M.P. Hertzberg, Concepts in Magnetic Resonance Part A, **18A**, 56 (2003)

[15] Nicole Pamme Lab Chip, **6**, 24 (2006)

[16] John V. Fahy, M.D., M.Sc. Asthma [Internet]. Version 11. Knol. 2008 Jul 28. available from: knol.google.com/k/john-v-fahy-m-d-m-sc/asthma/ei-9Hq9s/ASTp7w.

Separation from bulk solution

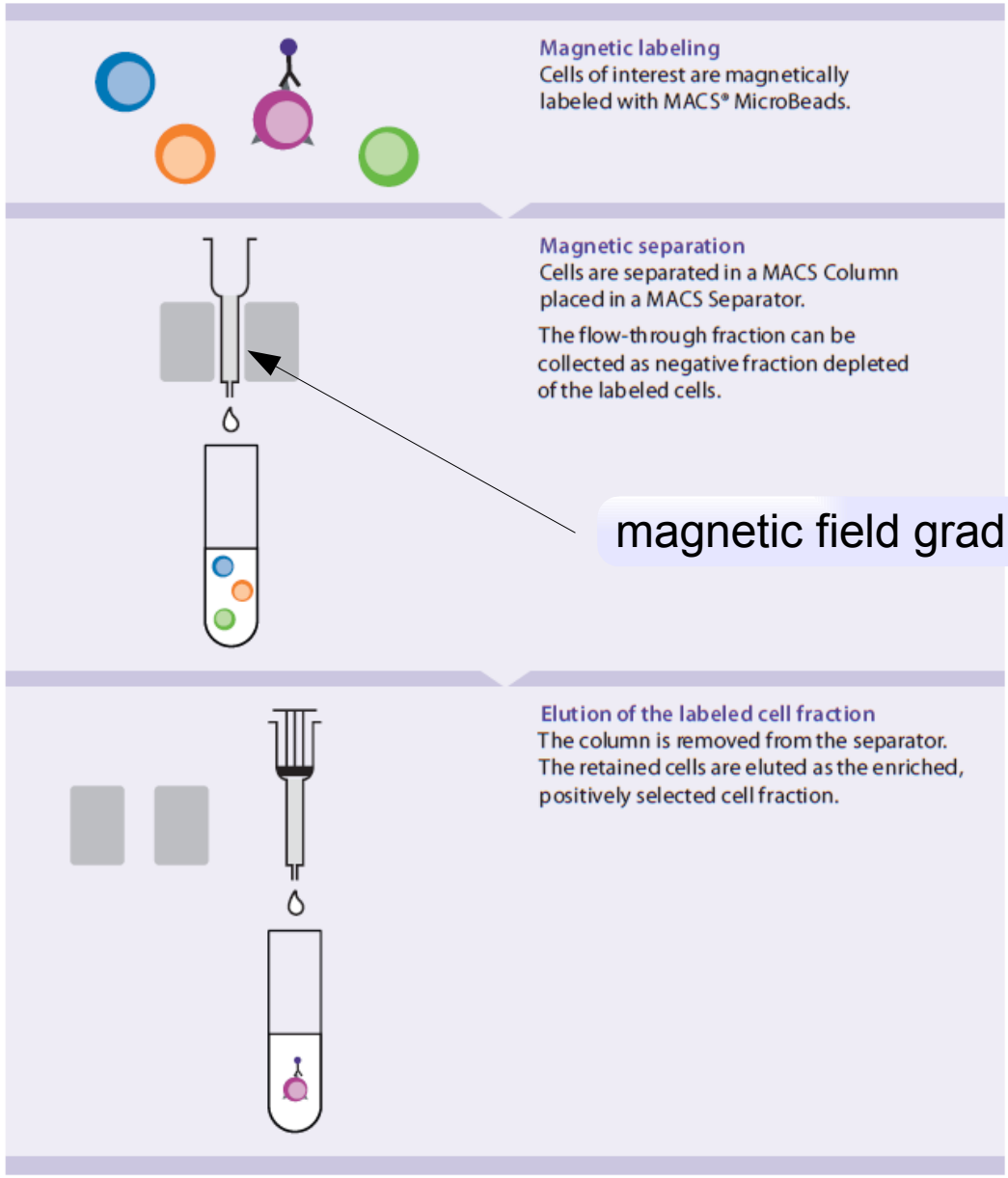

Figure 1: Positive selection strategy.

magnetic field gradient

Magnetic particles are functionalized to bind to specific cells or other chamicals

[9] Miltenyi_Biotec_Catalog2009.pdf, www.miltenyibiotec.com

Typical manipulation procedures

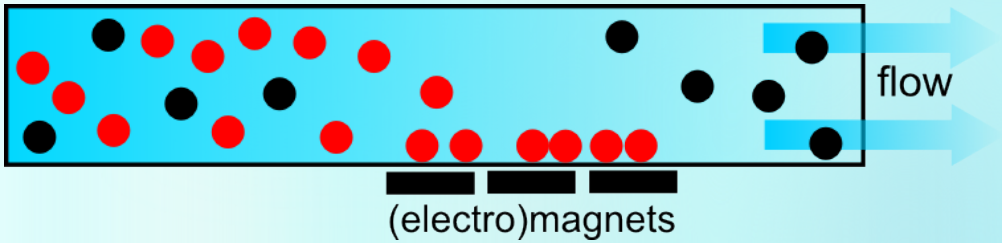

Magnetic particles captured - **separation**

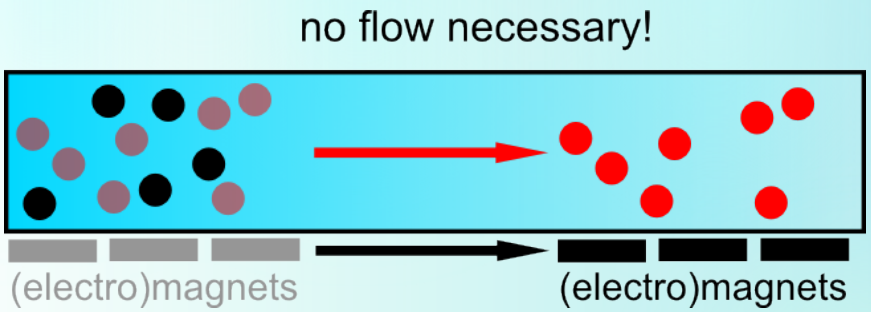

Magnetic particles moved - **transport**

Magnetophoresis - motion induced by a magnetic field on a particle of magnetic material in a fluid. [en.wiktionary.org]

Electrophoresis – used in forensic DNA analysis

[1] Martin A. M. Gijs, Frédéric Lacharme, and Ulrike Lehmann, Chamical Reviews **110**, 1518 (2010)

Forces in magnetic field – force field of a dipole on a paramagnet

$$E = -\vec{m}\cdot\vec{B}$$

$$\vec{F} = \nabla(\vec{m}\cdot\vec{B}) = -\vec{i}\,(m_x\frac{\partial B_x}{\partial x} + m_y\frac{\partial B_y}{\partial x} + m_z\frac{\partial B_z}{\partial x}) - \vec{j}\,(\ldots) - \ldots$$

$$\nabla\times\vec{B} = 0 \;:\qquad (\vec{J} + \frac{\partial \vec{D}}{\partial t} = 0 \;\leftarrow\; current\ free\ space\,,\ Maxwell)$$

$$\frac{\partial B_z}{\partial y} - \frac{\partial B_y}{\partial z} = 0 \qquad \frac{\partial B_x}{\partial z} - \frac{\partial B_z}{\partial x} = 0 \qquad \frac{\partial B_y}{\partial x} - \frac{\partial B_x}{\partial y} = 0$$

$$\vec{F} = -\vec{i}\,(m_x\frac{\partial B_x}{\partial x} + m_y\frac{\partial B_x}{\partial y} + m_z\frac{\partial B_x}{\partial z}) - \vec{j}\,(\ldots) - \ldots$$

$$\vec{F} = (\vec{m}\cdot\nabla)\vec{B}$$

...assuming constant gradient throughout the magnetic particle

Forces in magnetic field – force field of a dipole on a paramagnet

$$\vec{F} = (\vec{m}\cdot\nabla)\vec{B} = (\chi \frac{\vec{B}}{\mu_0} V\cdot\nabla)\vec{B} = \chi \frac{V}{\mu_0} \boxed{(\vec{B}\cdot\nabla)\vec{B}}$$

$$2\vec{B}\times(\underbrace{\cancel{\nabla\times\vec{B}}}_{0}) + 2\boxed{(\vec{B}\cdot\nabla)\vec{B}} = \nabla(\vec{B}\cdot\vec{B})$$

current free space,
no time-varying electric fields

$$\vec{F} = \frac{1}{2\mu_0}\chi V \nabla(B^2)$$

[12] Q. A. Pankhurst, J. Connolly, S. K. Jones, J. Dobson, J. Phys. D: Appl. Phys., **36**, R167 (2003)

Forces in magnetic field – force field of a dipole on a paramagnet

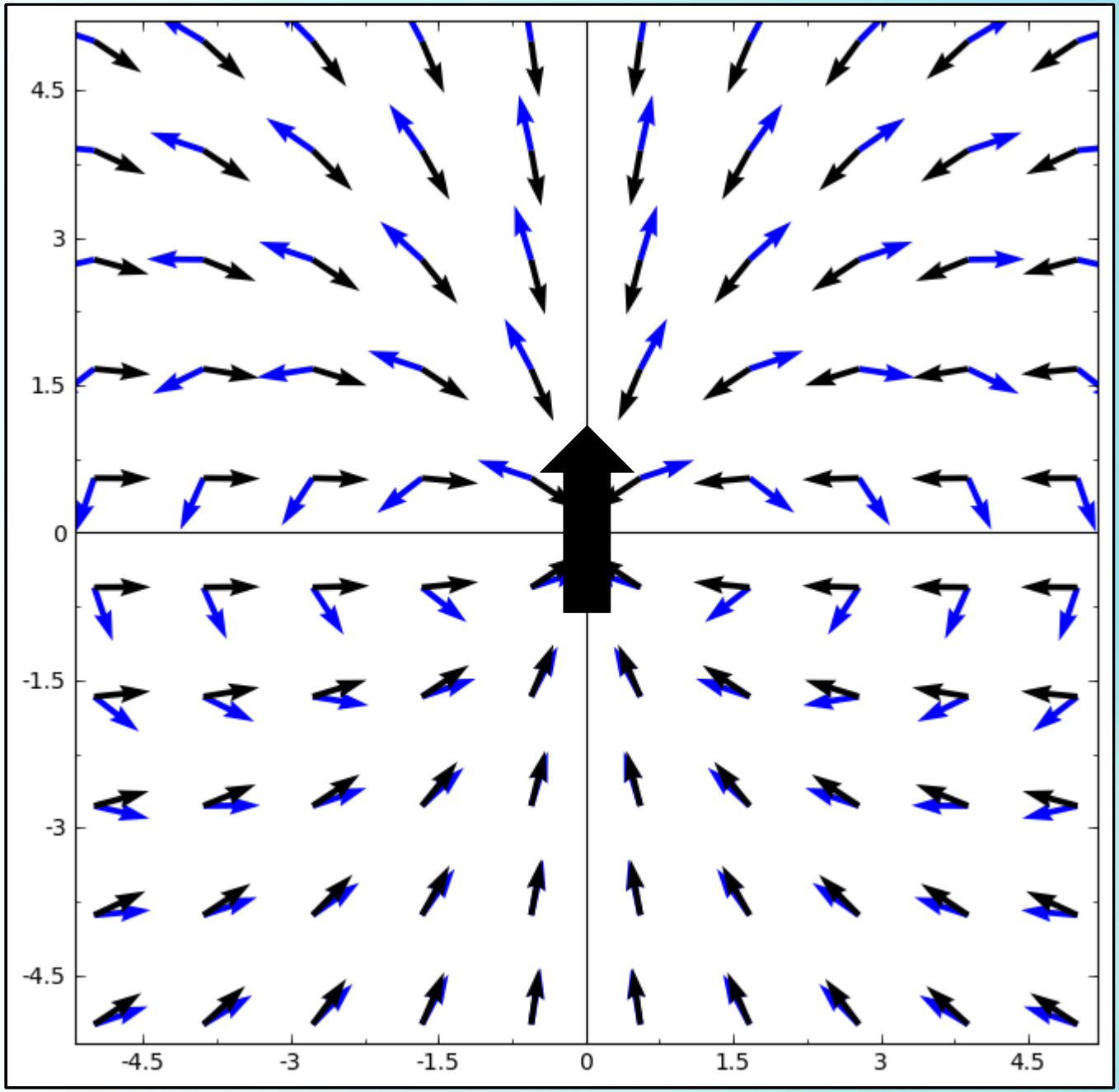

induction B

force

Force everywhere attractive !

Arrows show the directions of the fields
(not the magnitude!)

Forces in magnetic field – force field of a dipole on a paramagnet

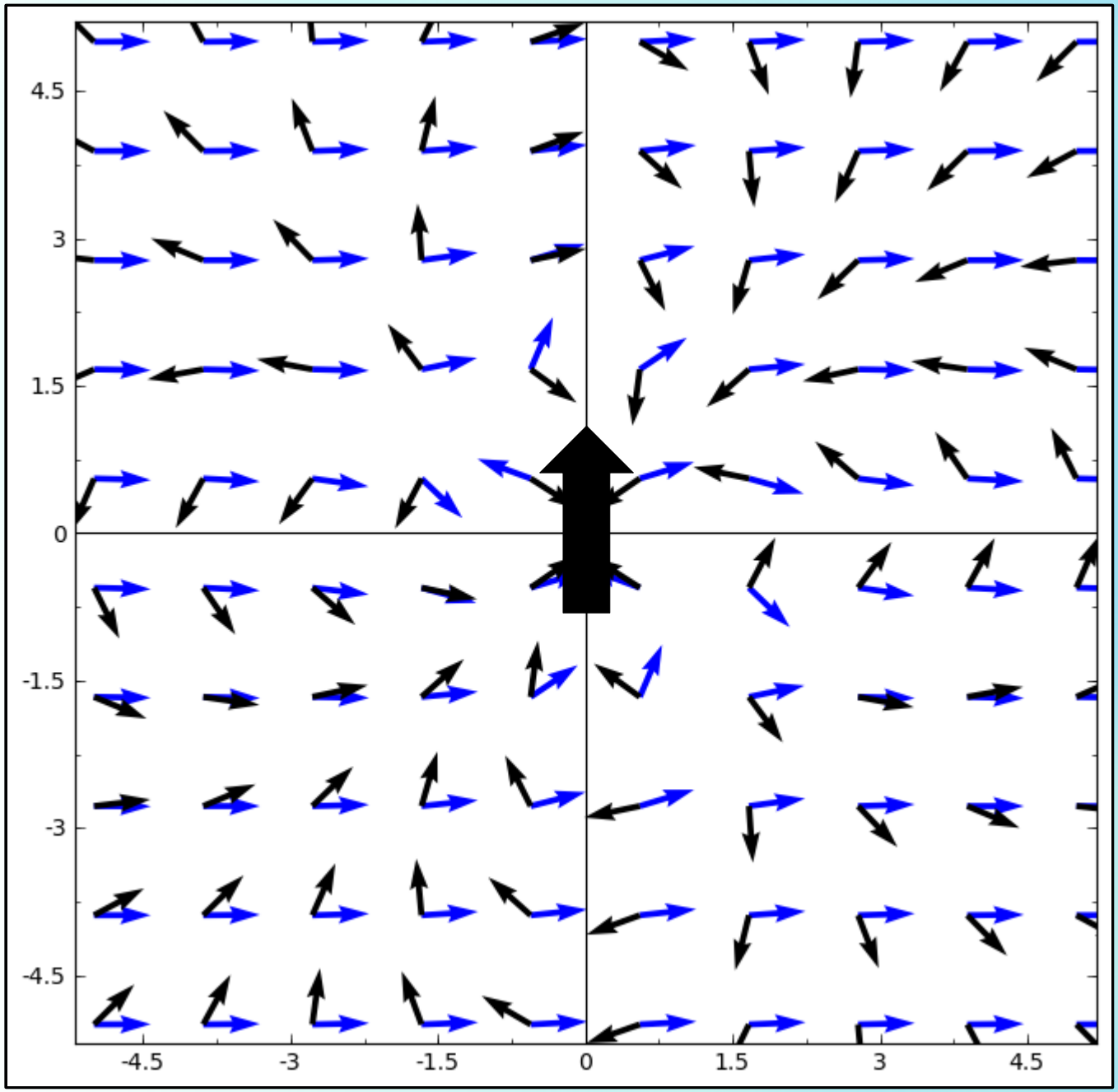

B_{ext}

Uniform external magnetic field increases force: the magnetic moment of particle is increased

induction B

force

Forces in magnetic field – force field of a dipole on a paramagnet

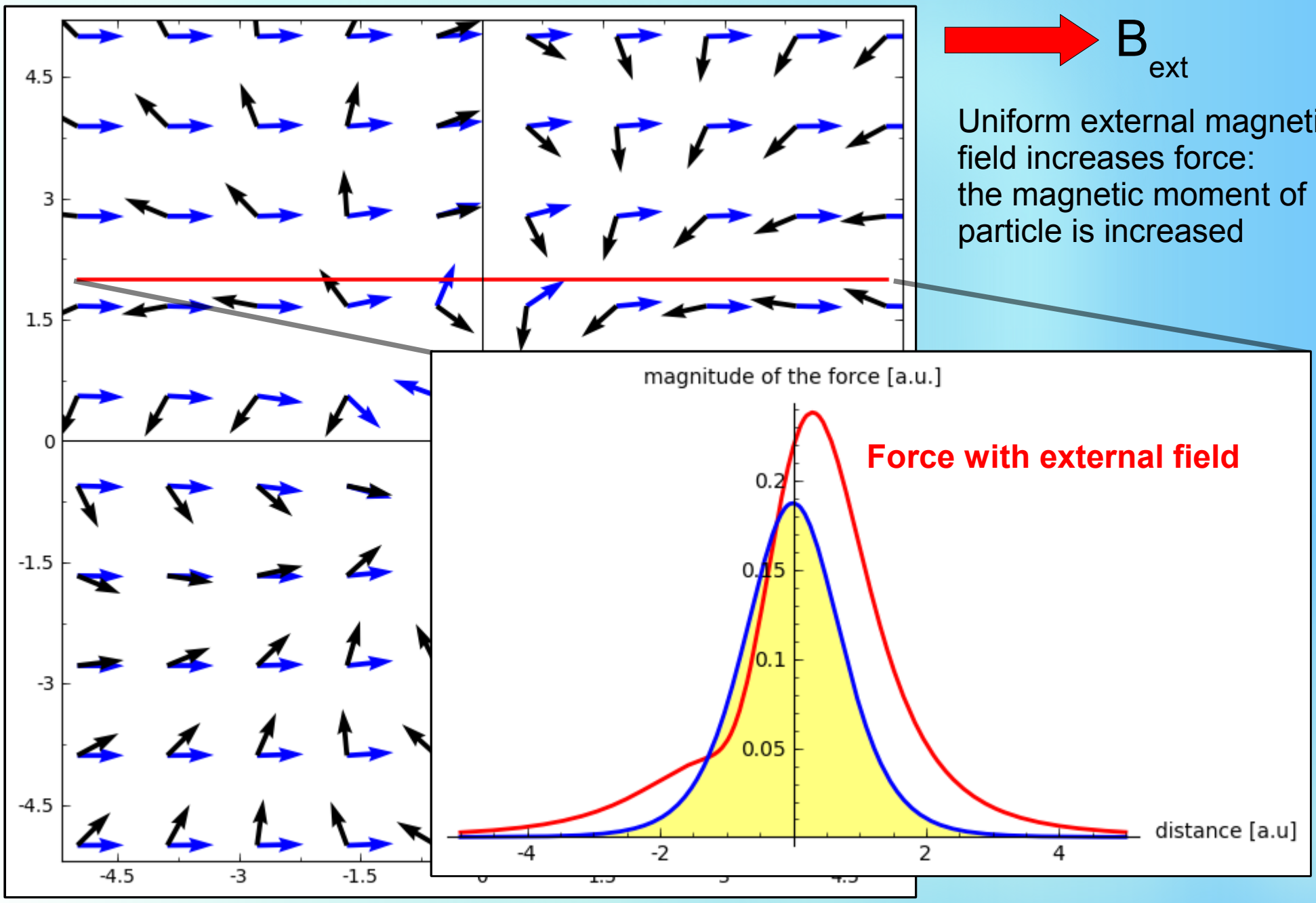

B_{ext}

Uniform external magnetic field increases force: the magnetic moment of particle is increased

Forces in magnetic field – force field of a dipole on a paramagnet

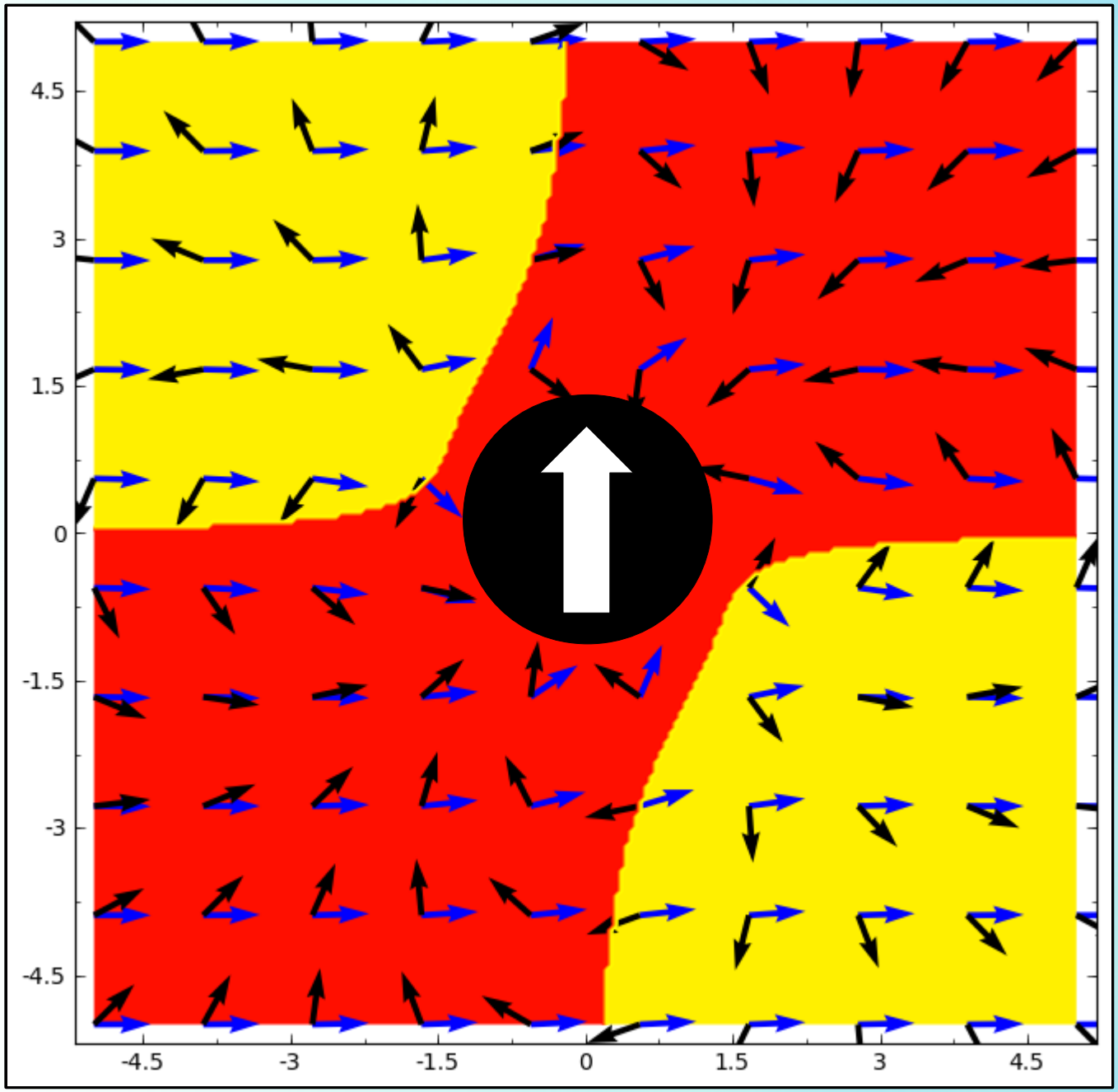

B_{ext}

Force repulsive or attractive !

Microfluidics

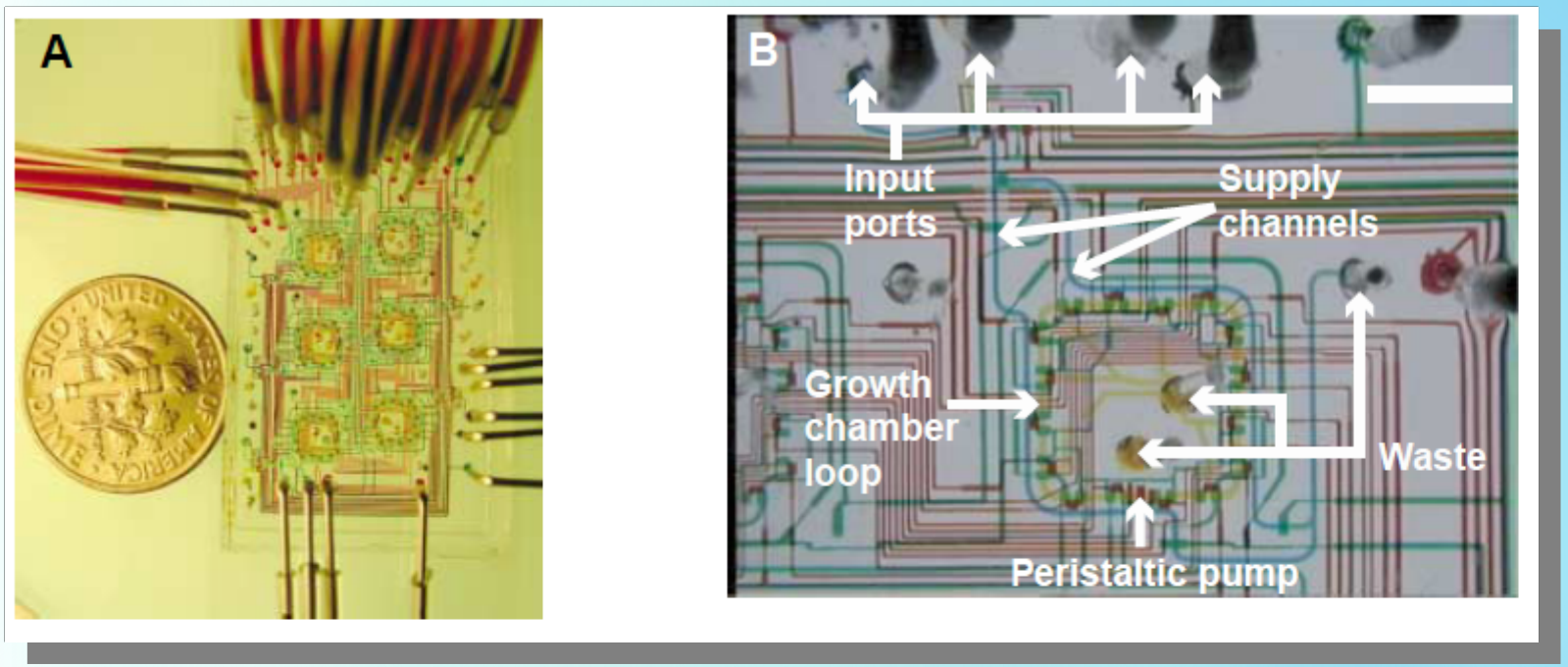

Fig. 1. (A) Optical micrograph showing six microchemostats that operate in parallel on a single chip. Various inputs have been loaded with food dyes to visualize channels and sub-elements of the microchemostats. The coin is 18 mm in diameter. (B) Optical micrograph showing a single microchemostat and its main components. Scale bar, 2 mm. (C) Schematic diagram of a microchemostat

- the possibility of using only minute quantities of sample and reagents (down to picoliters)
- fast reaction times

[18] F.K. Balagadde, Lingchong You, C.L. Hansen, F.H. Arnold, S.R. Quake, Science 309, 137 (2005)

Magnetophoresis of human blood cells

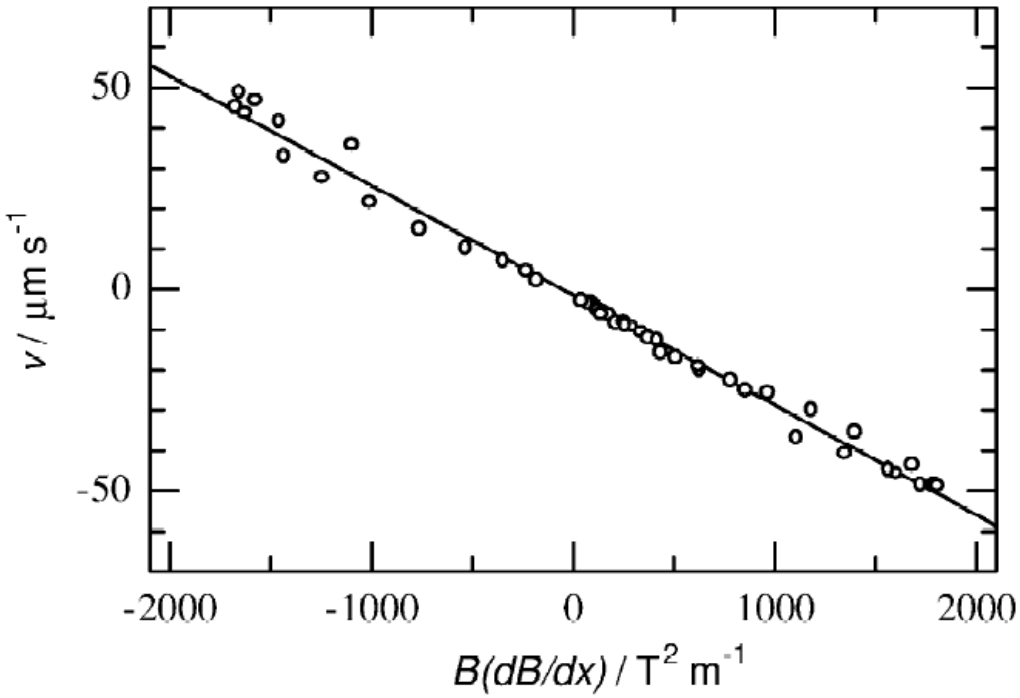

Fig. 5. Correlation between the velocity of red blood cells and the magnetophoretic intensity, $B(dB/dx)$. The slope of the line was used for the estimation of the volume magnetic susceptibility of red blood cells.

gap - 0.4mm

maximum B(dB/dx)=1800 T^2m^{-1}

red blood cells are diamagnetic (paramagnetic in deoxygenated state)

effective radius – 2.3 μm

$\chi = -9.035\times10^{-6}$

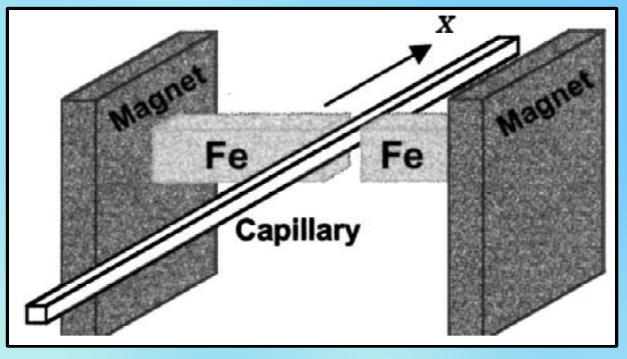

Fresh human blood was sampled just prior to use, from the author into a vial that contained EDTA aqueous solution to prevent the aggregation of the cells. One drop of blood sample was added to 10 ml of 0.1 *M* manganese(II) chloride solution, which is almost isotonic with real blood.

[17] H. Watarai, M. Namba, J. Chromatogr. A 961, 3 (2002)

Magnetophoresis of human blood cells

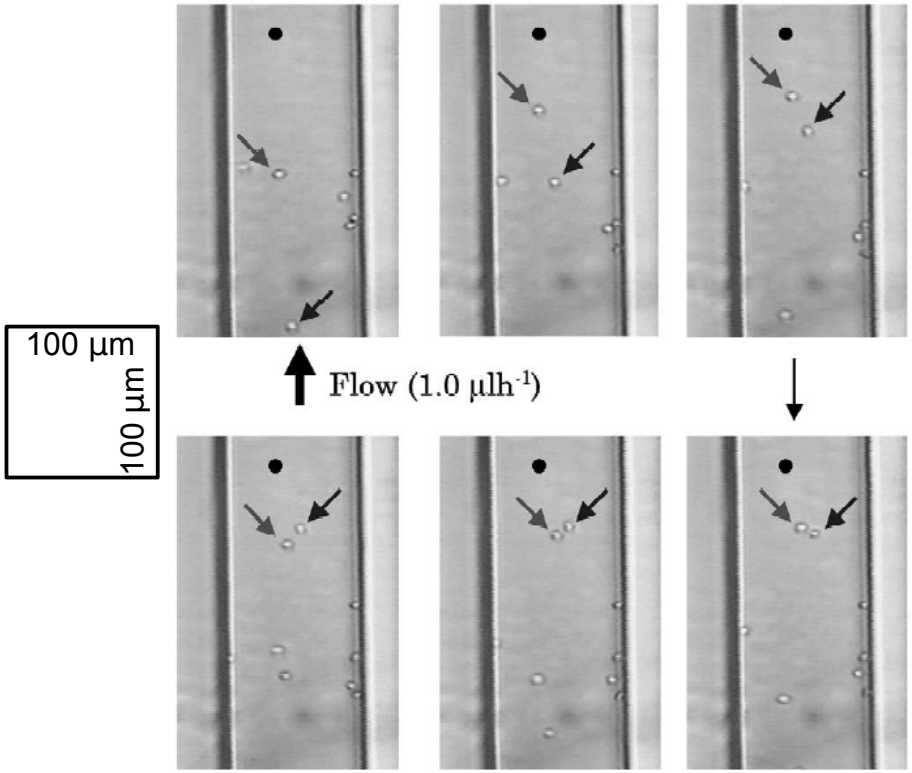

Fig. 6. Photographic representation of the magnetophoretic trapping of red blood cells at a flow-rate of 1.0 µl h^{-1} under the enhanced magnetic field. Pictures are shown at 3-s intervals from panels 1 to 6.

gap - 0.4mm

maximum B(dB/dx)=1800 T^2m^{-1}

red blood cells are diamagnetic (paramagnetic in deoxygenated state)

effective radius – 2.3 µm

$\chi = -9.035\times10^{-6}$

100% trapping of red blood cells in the counter-current flow mode for flow rates less than 1 µl h^{-1}.

[17] H. Watarai, M. Namba, J. Chromatogr. A 961, 3 (2002)

Magnetic beads

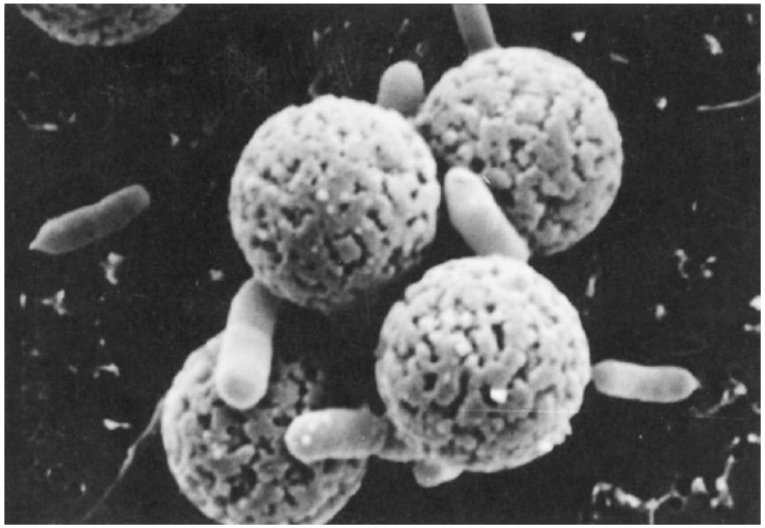

Fig. 2. An electron micrograph showing *E. coli* O157 bound to Dynabeads. Reproduced, with permission, from materials provided by Dynal, Oslo, Norway.

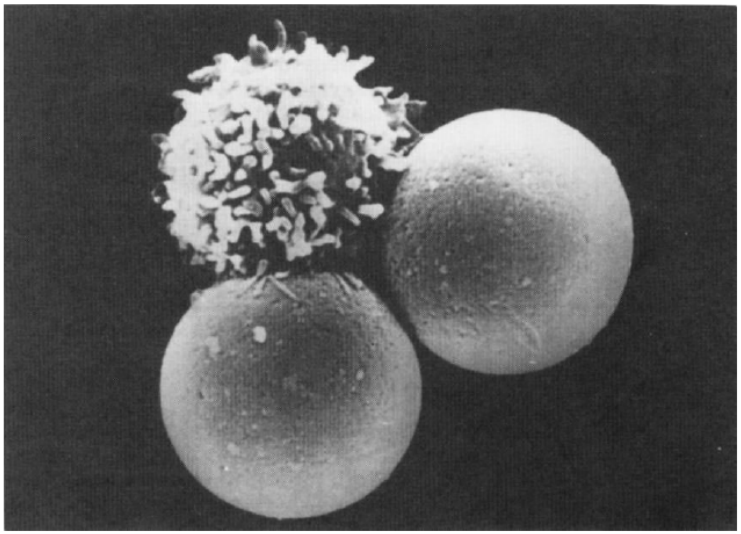

Fig. 3. An electron micrograph showing a T-lymphocyte bound to two Dynabeads M-450. Reproduced, with permission, from Ref. [8].

Diameters – several µm (Dynabeads M-270 D=2.8 µm)
Magnetic core – iron oxides
Susceptibility, χ=0.17 (Dynabeads M-270)

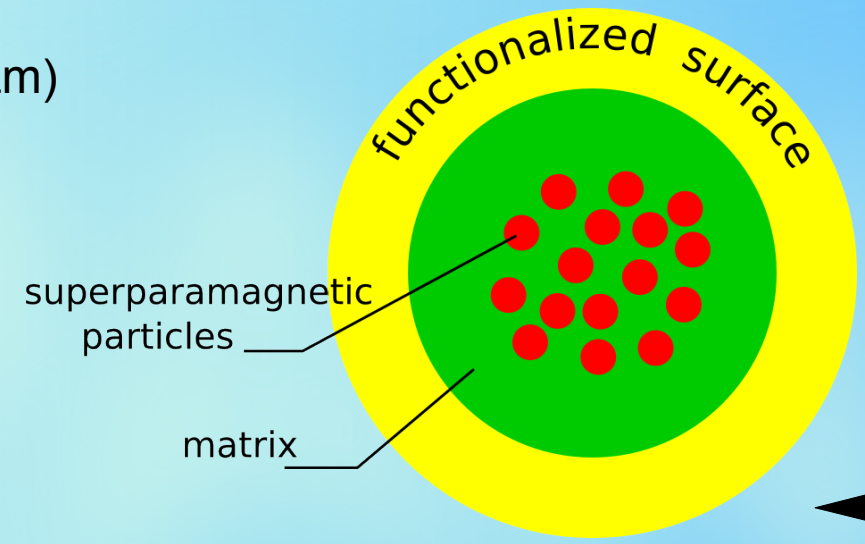

[11] I. Šafařik, M. Šafařıková, Journal of Chromatography B, **722**, 33–53 (1999)

Forces in magnetic field – force in medium with $\chi_{fluid} \neq 0$

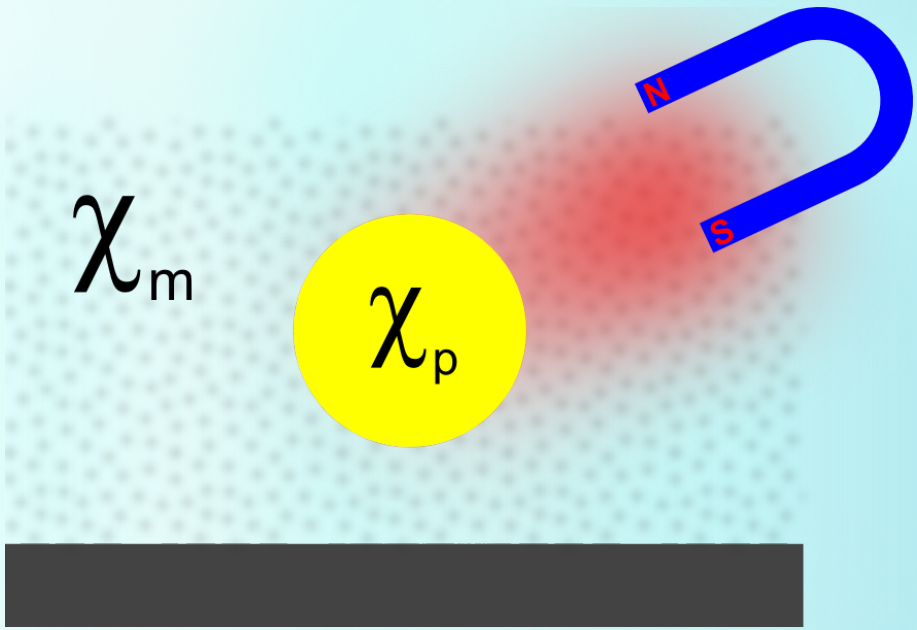

- Because of biocompatibility most magnetophoresis experiments are performed in water or aqueous solutions
- The magnetic susceptibility of water is small ($\chi = \mathbf{-9.035 \times 10^{-6}}$) compared to susceptibility of typical magnetic bead ($\chi_p \sim \mathbf{0.1}$)
- D-glucose: $\chi = -10.92 \times 10^{-6}$

$$\vec{F} = \frac{1}{2\mu_0}(\chi_p - \chi_m) V \nabla(B^2) \approx \frac{1}{2\mu_0}\chi_p V \nabla(B^2)$$

χ_p, χ_m susceptibilities of particle and medium (e.g. water)

[15] Nicole Pamme, Lab Chip, **6**, 24 (2006)

[14] P.W. Kuchel et al., Concepts in Magnetic Resonance Part A, **18A**, 56 (2003)

“Early days” of particle manipulation

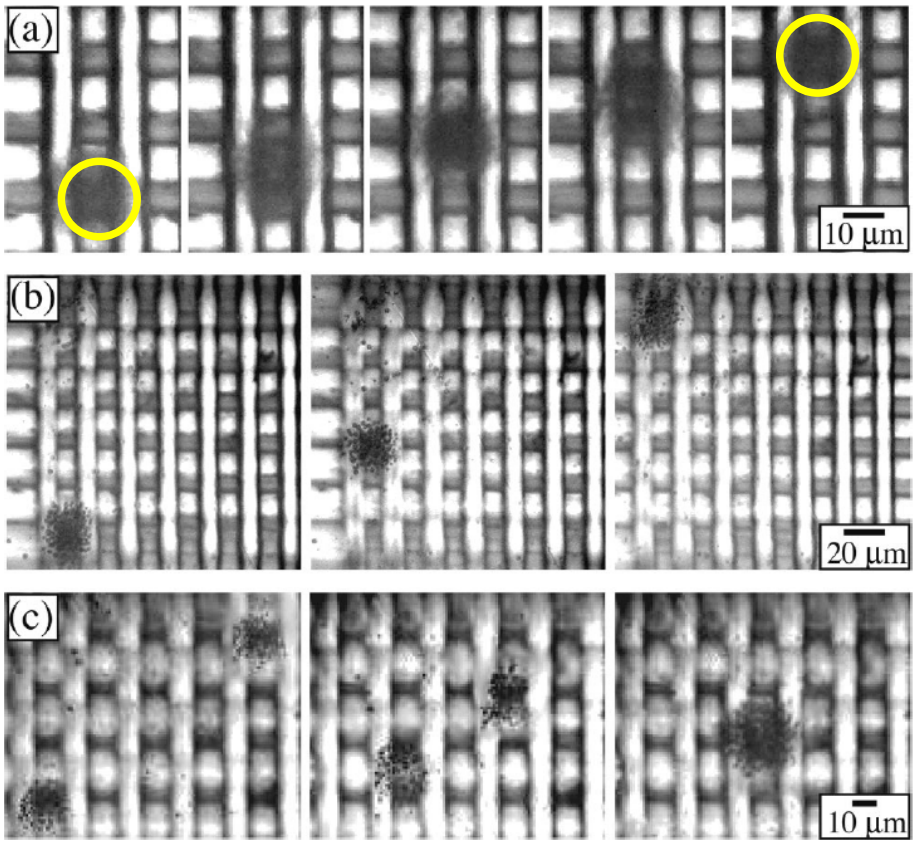

FIG. 4. (a) Demonstration of moving a group of superparamagnetic particles over two wires of a microelectromagnet matrix. The wire currents were adjusted so they continuously move particles by increments that are less than the wire spacing. The size of the particle group is broader above the wire, in agreement with the simulation in Fig. 2(b). (b) A group of particles is moved vertically by the matrix over a longer range of five wire spacings. (c) Two groups of particles are moved diagonally to join them together at a single location. Particles can be moved diagonally at any angle. These experimental results agree well with the motion of peaks of the magnetic field magnitude shown in Fig. 2. Current was passed through all 14 wires for the demonstrations shown.

- magnetic particles diameter ~1-2 μm
- superparamagnetic core (The particles are 1–20 nm magnetite nanoparticles coated with a polymer composed of polystyrene and carboxylic acid, suspended in a water based solution.)
- very precise positioning- $\Delta x \approx 10$ μm
- complicated wiring: currents provide the magnetic field

Practical realization of particle transport

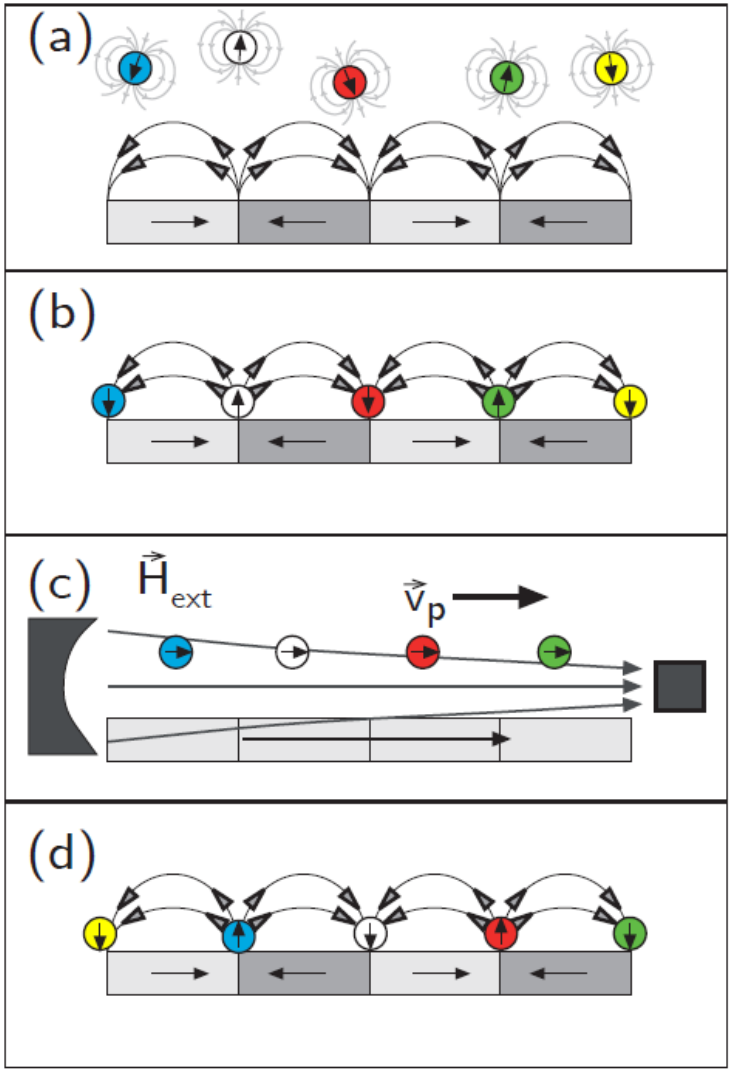

Abb. 5.16: Schematische Darstellung des Konzeptes zum Partikeltransport. (a) Die magnetischen Momente der Partikel richten sich in den Streufeldern der magnetisch strukturierten Probe aus. (b) Die Partikel lagern sich aufgrund der magnetischen Kräfte an den Orten hoher magnetischer Streufelder, d.h. an den Domänenwänden an. (c) Ein externes inhomogenes Magnetfeld sättigt das Substrat und richtet die magnetischen Momente der Partikel neu aus, die dann dem Feldgradienten folgend transportiert werden. (d) Nach Abschalten des externen Feldes lagern sich die Partikel wieder an den Streufeldern der Probe an. Die magnetischen Streufelder der Partikel sind zugunsten der besseren Übersicht nur in (a) eingezeichnet.

Magnetic patterning by 10 keV He^+ bombardment:

change of the exchange bias in **IrMn/NiFe**

Step-wise controllable transport

[8] Tanja Weis, Dissertation, Kassel 2009

Practical realization of particle transport

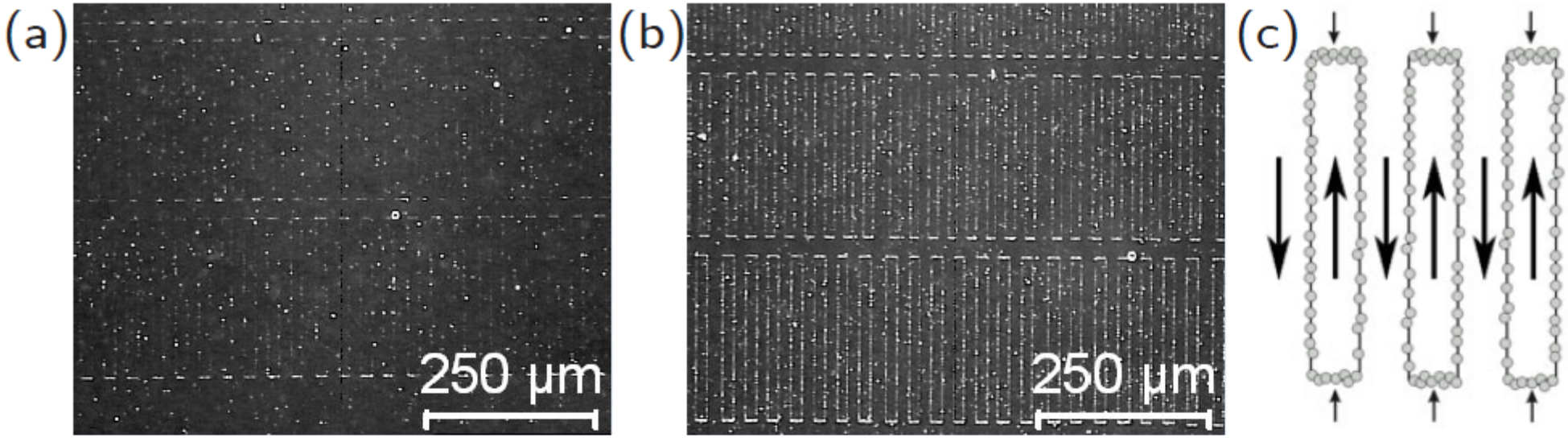

Abb. 5.15: Lichtmikroskopische Aufnahmen von Proben mit magnetischen abgeschlossenen Rechtecken (obere Reihe: 15 μm Breite, 200 μm Länge) nach Aufbringen der 250 nm-Partikel mit der Volumenmethode in Lösung in 100-facher Vergrößerung nach 15 min (a) und nach 60 min (b). Schematische Darstellung der Anlagerung der Partikel an den Domänengrenzen (c). Die Pfeile geben die alternierenden Magnetisierungsrichtungen in den Streifen wieder.

Accumulation of magnetic particles on domain walls

[8] Tanja Weis, Dissertation, Kassel 2009

Practical realization of particle transport

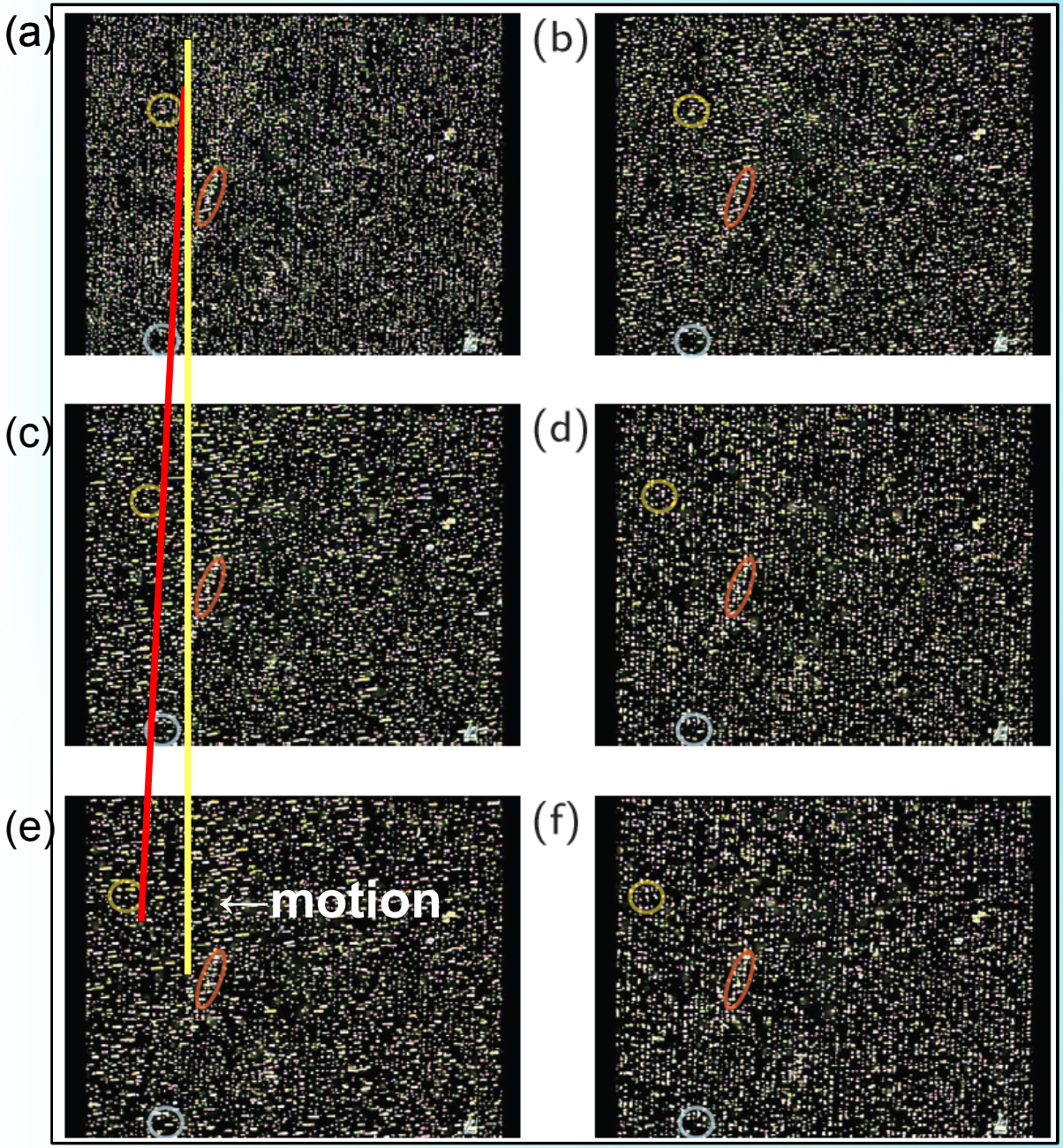

Abb. 5.24: Standbilder aus dem Video 5, das in 100-facher Vergrößerung zum Nachweis des Transports der Partikel (**d=2 µm**, Konzentration c = 2.2 x10^4 Partikel/µl) auf magnetisch in 5 µm breite Streifen (Periodizität 10 µm) strukturiertem EB-Substrat (IrMn (11,6nm) / NiFe (7,8nm), vgl. Kap. 5.1.3) im gepulsten Magnetfeld (Pulsdauer 2500 ms, H = 0 und -60 kA/m, dH/dx = 0 und 3.5x10^5 A/m^2 bei Schaltung 1) aufgenommen wurde. Die Bilder (a) bis (f) enstanden im Abstand von jeweils 2 s. (a) Direkt nach dem Aufbringen der Partikel; es lag noch kein Feld an. (b) und (c) Während des ersten Feldpulses. (d) Zwischen Feldpuls 1 und 2. (e) Während des zweiten Feldpulses. (f) Nach dem zweiten Feldpuls. Zur leichteren Zuordnung sind in den verschiedenen Bildern die selben Partikel(-gruppen) gleichfarbig markiert. Die Bilder zeigen jeweils einen Ausschnitt von **580 x 430 µm**.

Controllable transport with 5µm step!

movie

[8] Tanja Weis, Dissertation, Kassel 2009

Microseparator (model)

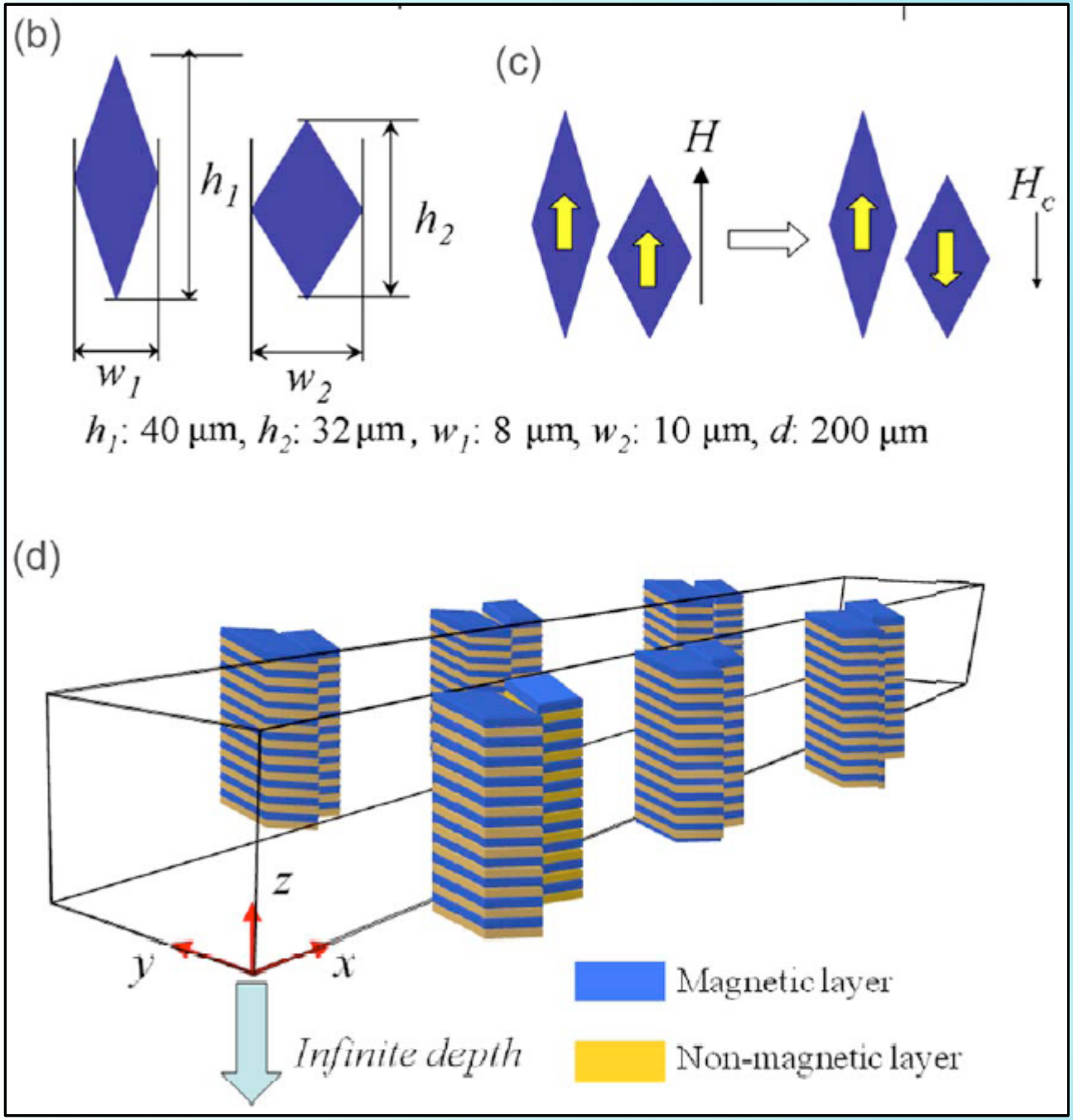

- multilayer stacks provide magnetic field gradient
- shape dependent coercive field value (H_c)
- velocity of the suspended solution is set as **1 mm/s** at the channel inlet
- **power consumption reduced**
- simulation with COMSOL (hydrodynamic drag force included)

[2] Reprinted with permission from Chiun-Peng Lee and Mei_Feng Lai, J. Appl. Phys. 107, 09B524 (2010) Copyright 2010, American Institute of Physics.

Microseparator (model)

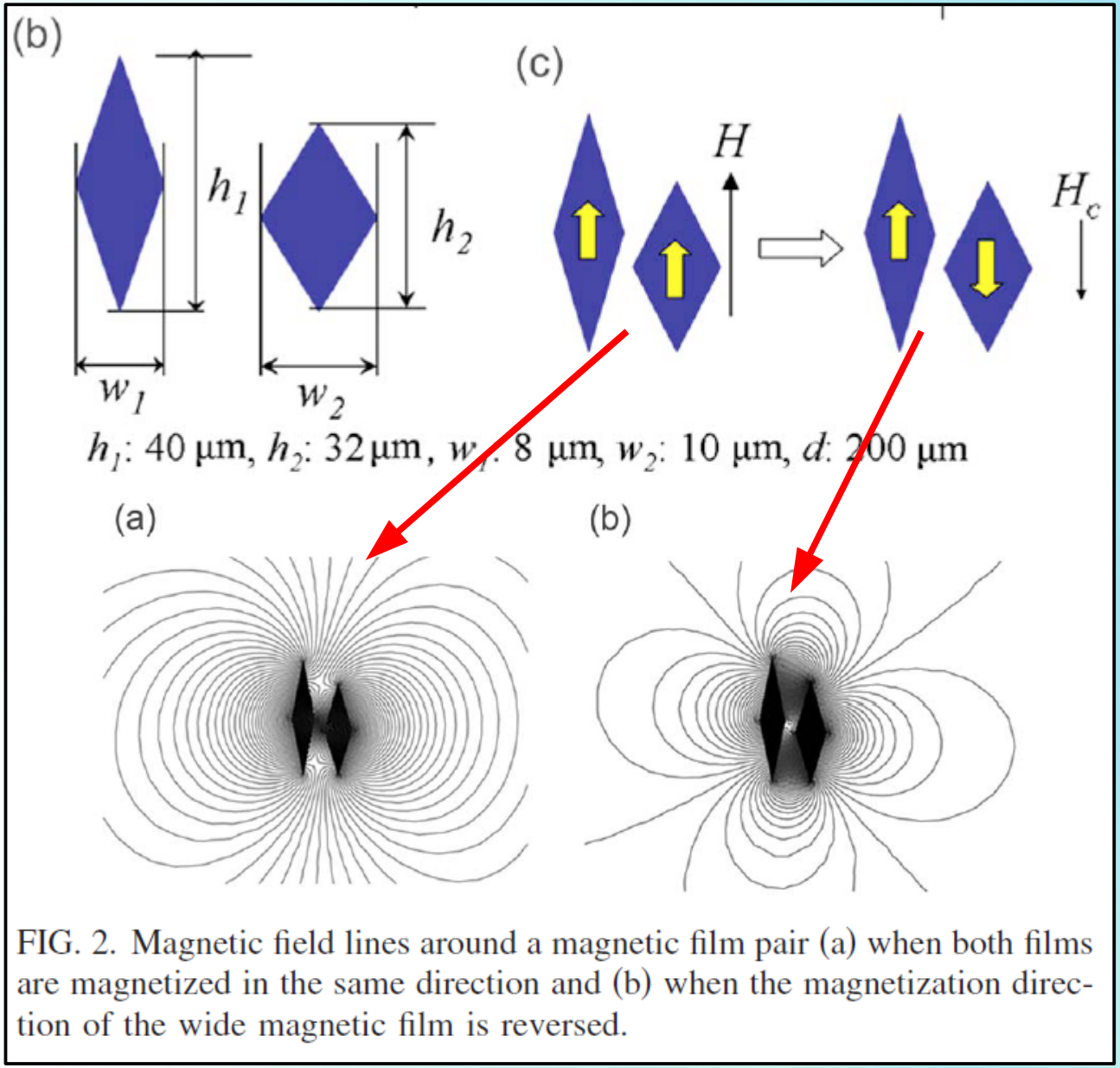

FIG. 2. Magnetic field lines around a magnetic film pair (a) when both films are magnetized in the same direction and (b) when the magnetization direction of the wide magnetic film is reversed.

parallel configuration-fields are significant over large distances

antiparallel configuration-significant fields only in the vicinity of the stacks

Microseparator (model)

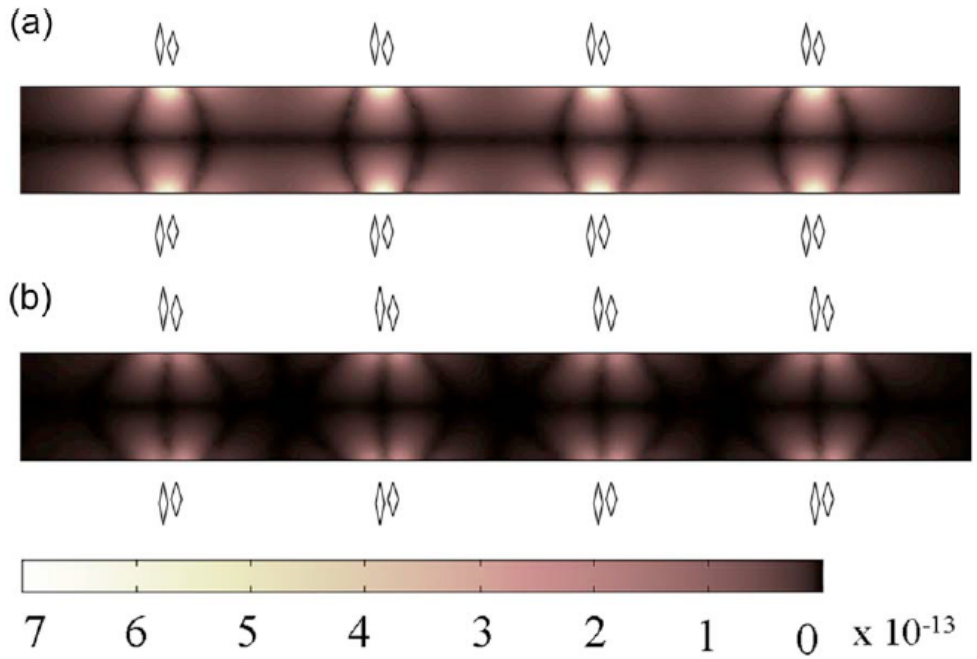

FIG. 3. (Color online) The y-component distribution of the magnetic force exerting on magnetic particles (a) when all magnetic films are magnetized in the same direction and (b) when the magnetizations of the wide magnetic films are reversed. The unit of the color bar is N.

parallel configuration

antiparallel configuration

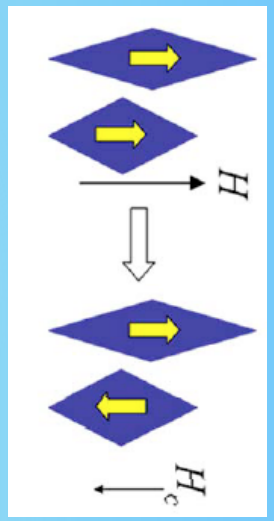

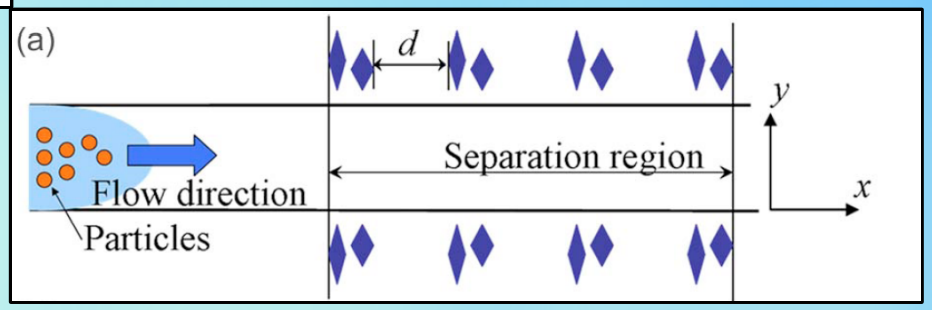

d=200 μm

particle diameter=1 μm, ρ=1400 kg m^{-3},

magnetic force=3x10^{-13} N:

acceleration a≈42 g !

Viscous drag force

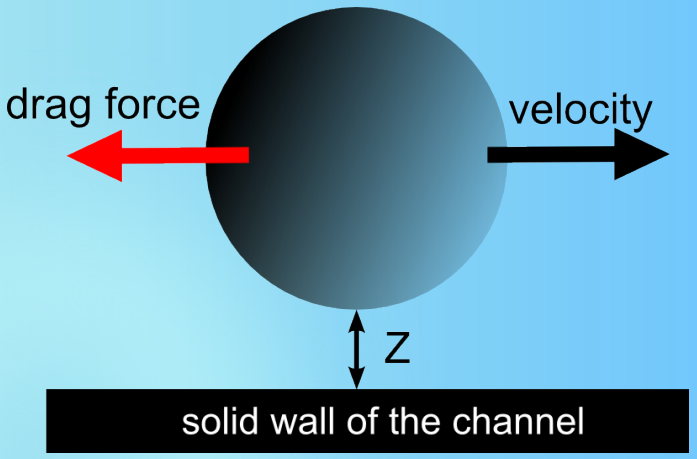

$$F_d = 6\pi\eta r \Delta v f_D$$

$$f_D = \left(1 - \frac{9}{16}\left(\frac{r}{r+z}\right) + \frac{1}{8}\left(\frac{r}{r+z}\right)^3 - \frac{45}{256}\left(\frac{r}{r+z}\right)^4 - \frac{1}{16}\left(\frac{r}{r+z}\right)^5\right)$$

$\eta - viscosity\,(8.9\times10^{-4}\,N\,s\,m^{-2}\ for\ water)$

$f_D - drag\ coefficient$

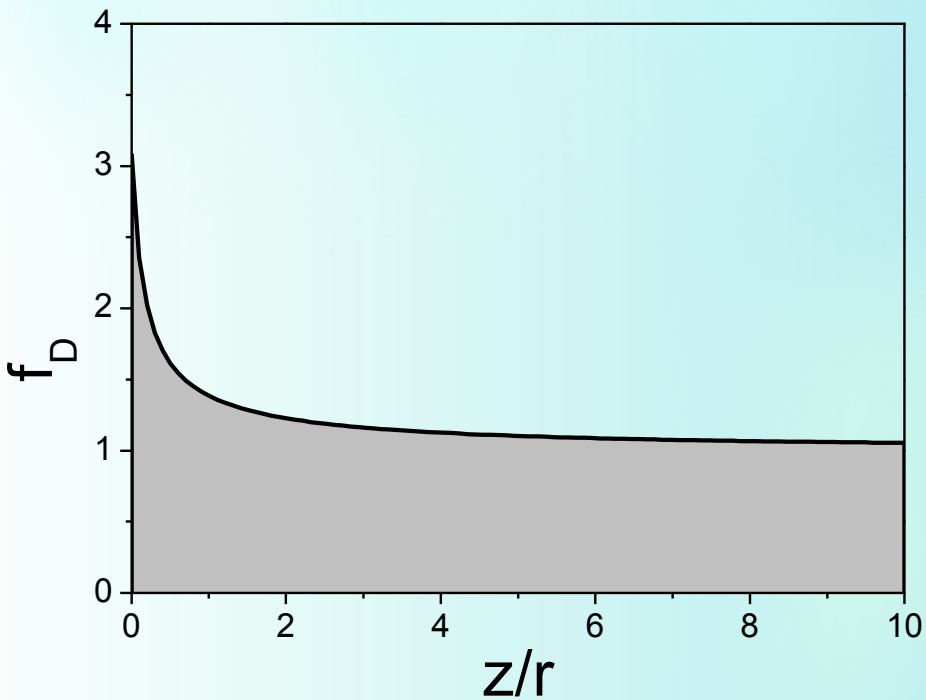

The influence of channel walls is significant for z/r approximately less than 2.

Viscous force is position dependent!

[1] Martin A. M. Gijs, Frédéric Lacharme, and Ulrike Lehmann, Chamical Reviews **110**, 1518 (2010)

Viscous drag force

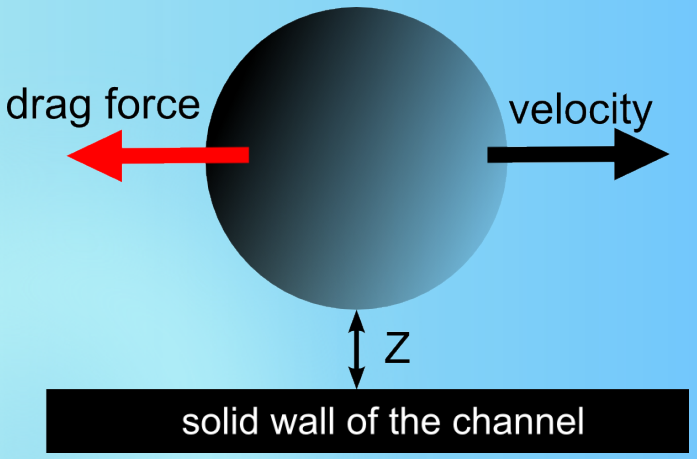

$$F_d = 6\pi\eta r \Delta v f_D$$

$$f_D = \left(1 - \frac{9}{16}\left(\frac{r}{r+z}\right) + \frac{1}{8}\left(\frac{r}{r+z}\right)^3 - \frac{45}{256}\left(\frac{r}{r+z}\right)^4 - \frac{1}{16}\left(\frac{r}{r+z}\right)^5\right)$$

$\eta - viscosity\,(8.9\times10^{-4}\,N\,s\,m^{-2}\ for\ water)$

$f_D - drag\ coefficient$

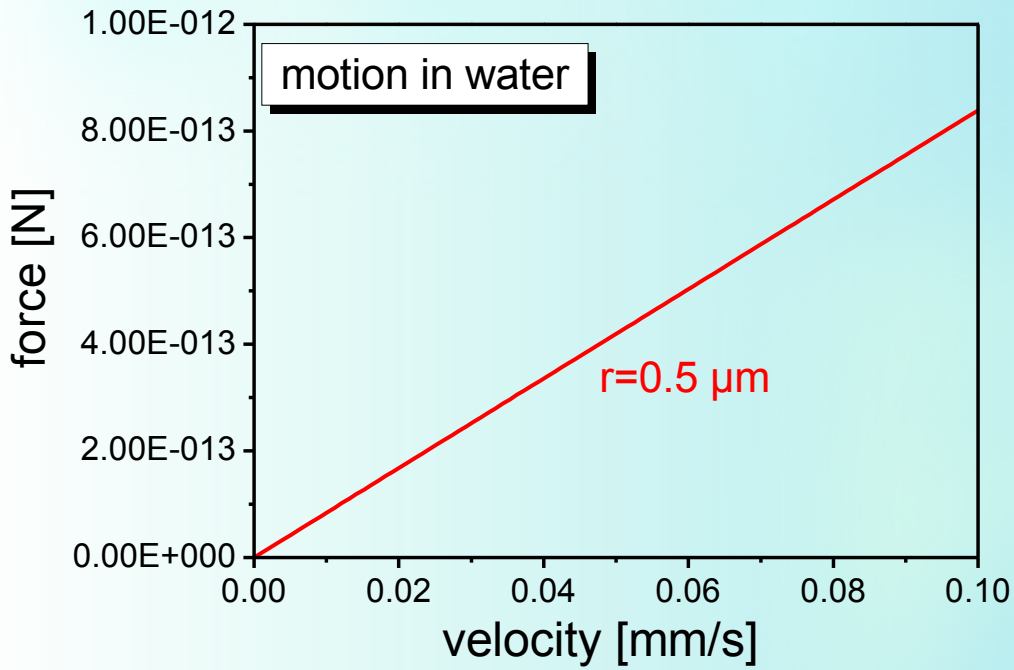

Velocity of the particles in the suspension is limited primarily by the viscous drag.

Viscous drag is approx. proportional to the particle diameter.

[1] Martin A. M. Gijs, Frédéric Lacharme, and Ulrike Lehmann, Chamical Reviews **110**, 1518 (2010)

Sinking speed – gravitation, buoyancy and viscous drag

$$F_d = 6\pi\eta r \Delta v f_D = g V(\rho_{bead} - \rho_{fluid})$$

$$f_D = 1$$

$$\eta - viscosity\,(8.9\times10^{-4}\,N\,s\,m^{-2}\ for\ water)$$

$$f_D - drag\ coefficient$$

$$\rho_{bead} \approx 1.8\,g/cm^3 \quad (for\ MyOne\ Dynabeads)$$

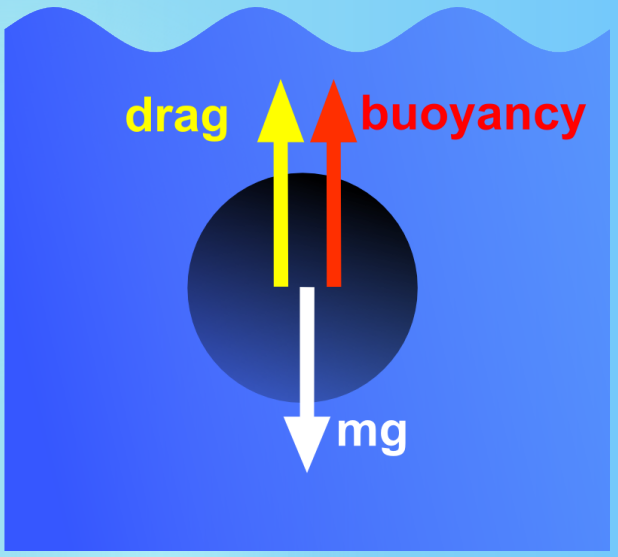

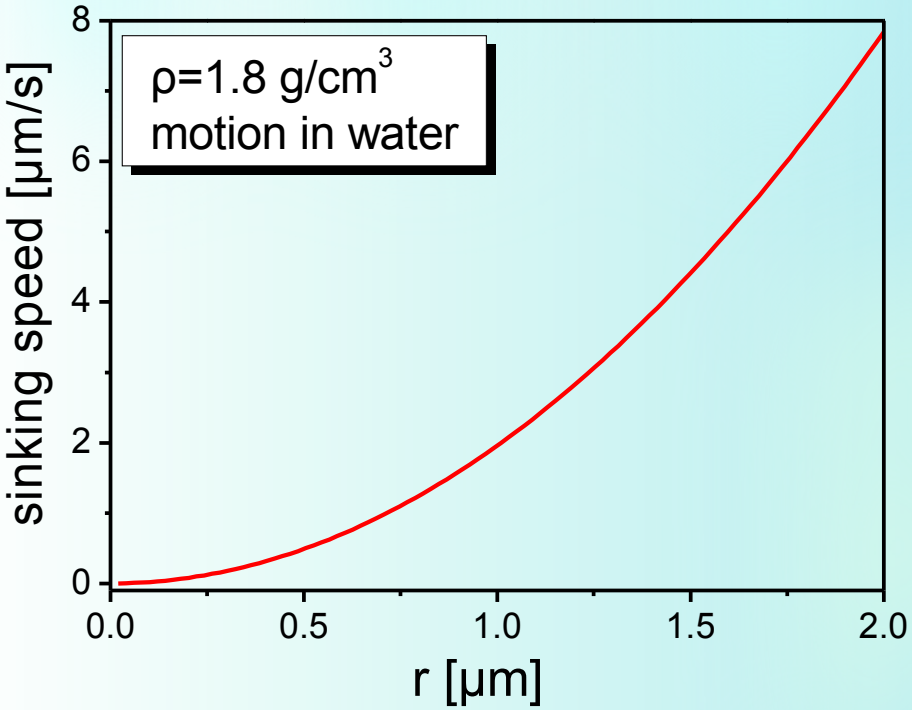

Smaller particles sink much slower
$v_{sink} \sim r^2$
For typical magnetic beads
$v_{sink} \approx 0.5$ µm/s

[1] Martin A. M. Gijs, Frédéric Lacharme, and Ulrike Lehmann, Chamical Reviews **110**, 1518 (2010)

Brownian forces

Stokes-Einstein relation:

$$D = \frac{k_B T}{6 \pi \eta r_{bead}}$$

$D - difussion \;\; coefficient$

$\eta - viscosity \left(8.9 \times 10^{-4} N\, s\, m^{-2} \; for\, water\right)$

Mean square displacement of Brownian particle:

$$\langle r^2 \rangle = 6\, D\, t$$

$t - time$

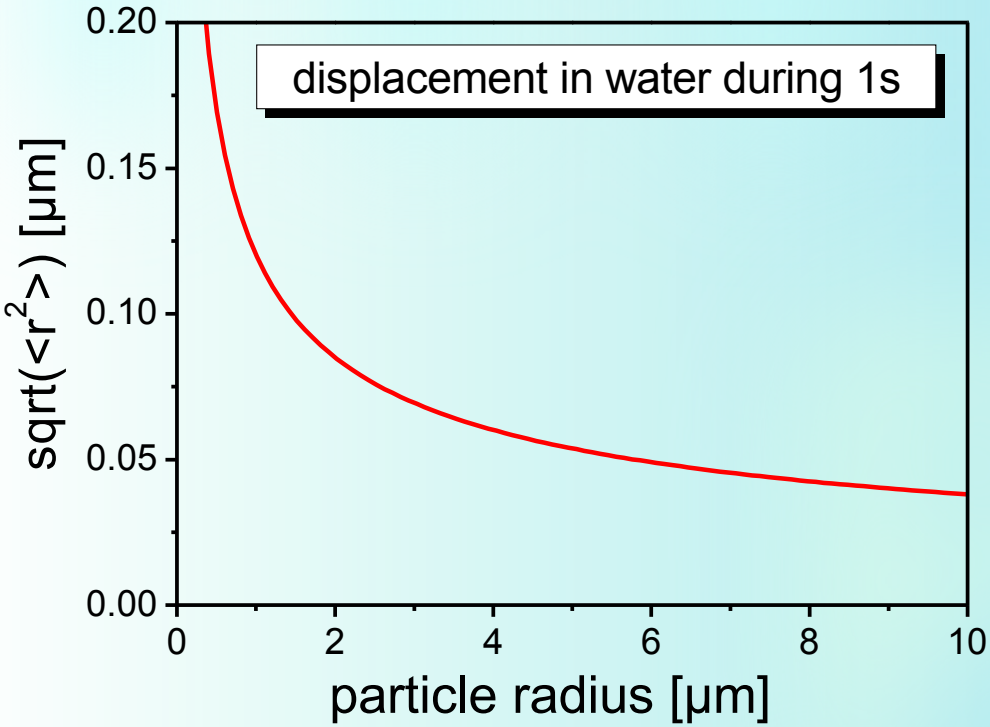

When the magnetic particles are larger than ~1 µm the Brownian forces are irrelevant.

sqrt(6*(
1.38*10^(-23)*293/
(6*Pi*x*8.9*10^(-4))
)*1)

[1] Martin A. M. Gijs, Frédéric Lacharme, and Ulrike Lehmann, Chamical Reviews **110**, 1518 (2010)

Microseparator (model)

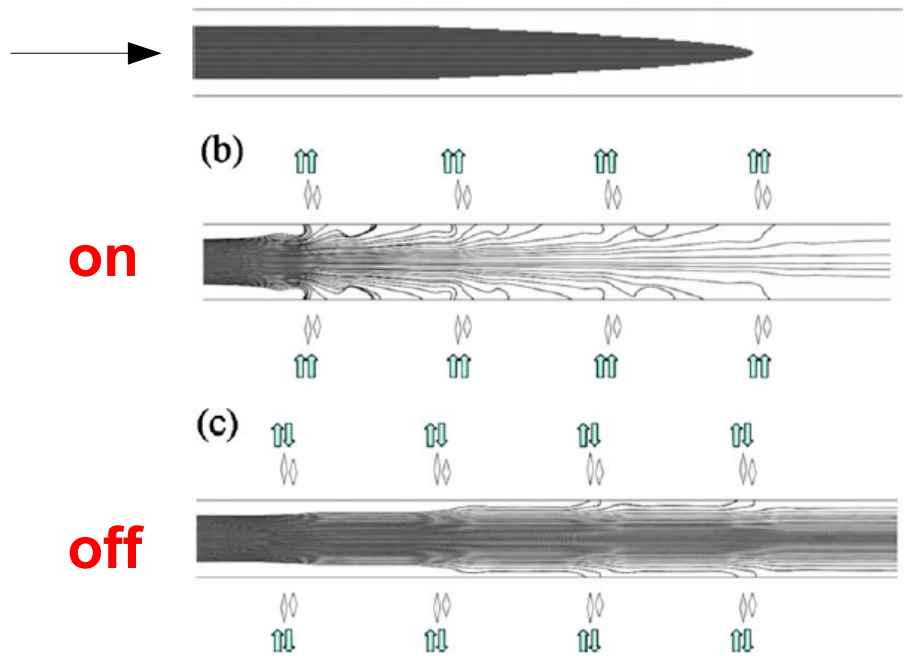

FIG. 4. (Color online) Trajectories of magnetic particles when (a) there are no magnetic films, (b) when all magnetic films are magnetized in the same direction, and (c) when the magnetizations of the wide magnetic films are reversed. The arrows indicate the magnetization directions of the magnetic films.

Separation rate = 87.5%

Separation rate = 20%

- 2D simulation
- 40 particles
- particles M_S= 15 kA/m
- separator M_S= 64 kA/m (magnetic films)

could be useful for "biomicrofluidic applications using magnetic particles"

[2] Reprinted with permission from Chiun-Peng Lee and Mei_Feng Lai, J. Appl. Phys. 107, 09B524 (2010) Copyright 2010, American Institute of Physics.

Colloidal magnetic shift register

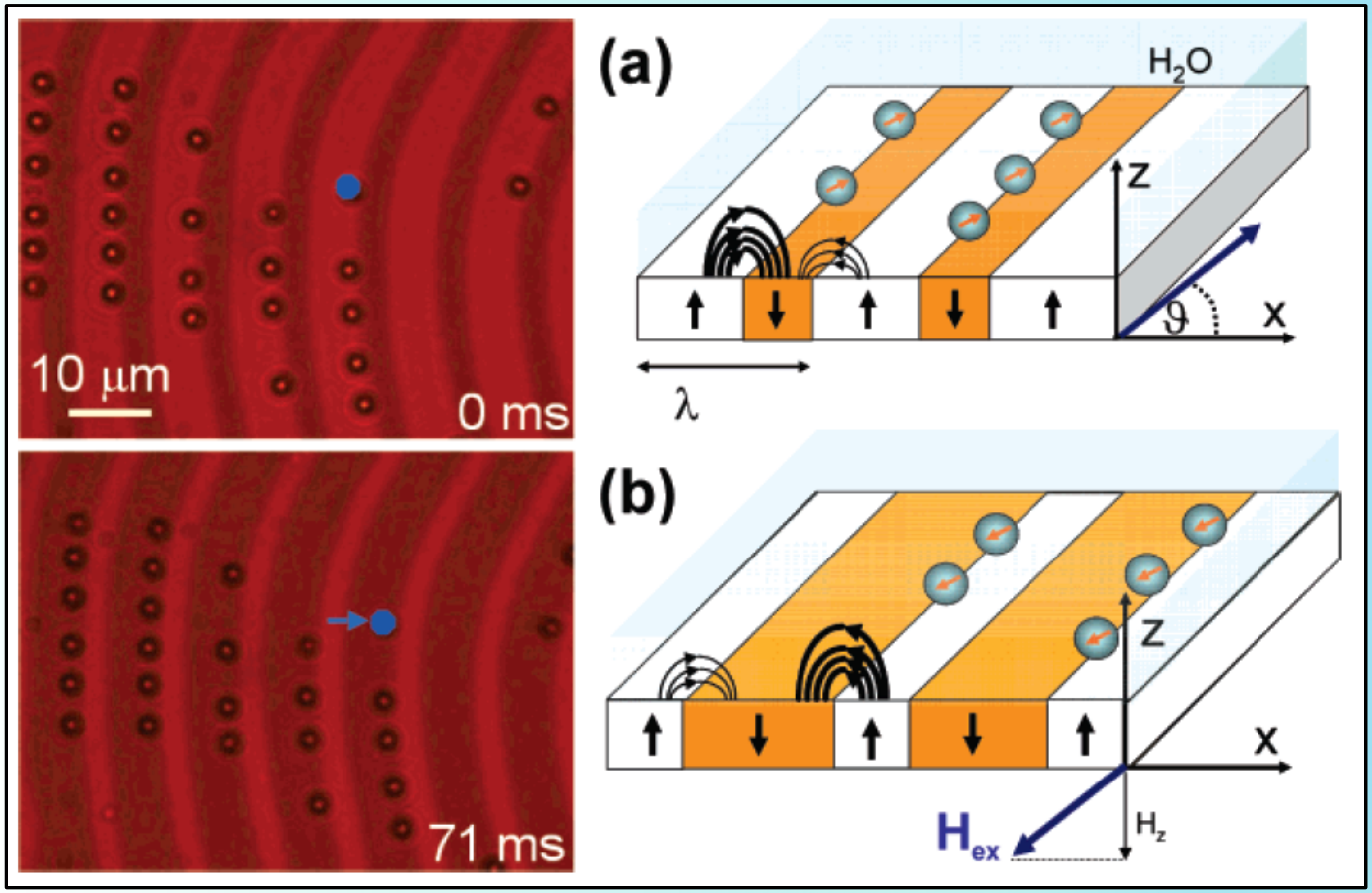

- stripe pattern on 5µm thick $Y_{2.5}Bi_{0.5}Fe_{5-q}Ga_qO_{12}$ (q=0.5-1)
- M_S= 17 kA/m
- liquid phase epitaxy
- d= **2.8** µm± 0.1µm; Susceptibility, χ=0.17 (Dynabeads M-270)

[5] Reprinted with permission from P. Tierno, S. V. Reddy, J. Yuan, T. H. Johansen, and T. M. Fischer, J. Phys. Chem. B , 111, 13479 (2007). Copyright 2007 American Chemical Society.

Colloidal magnetic shift register

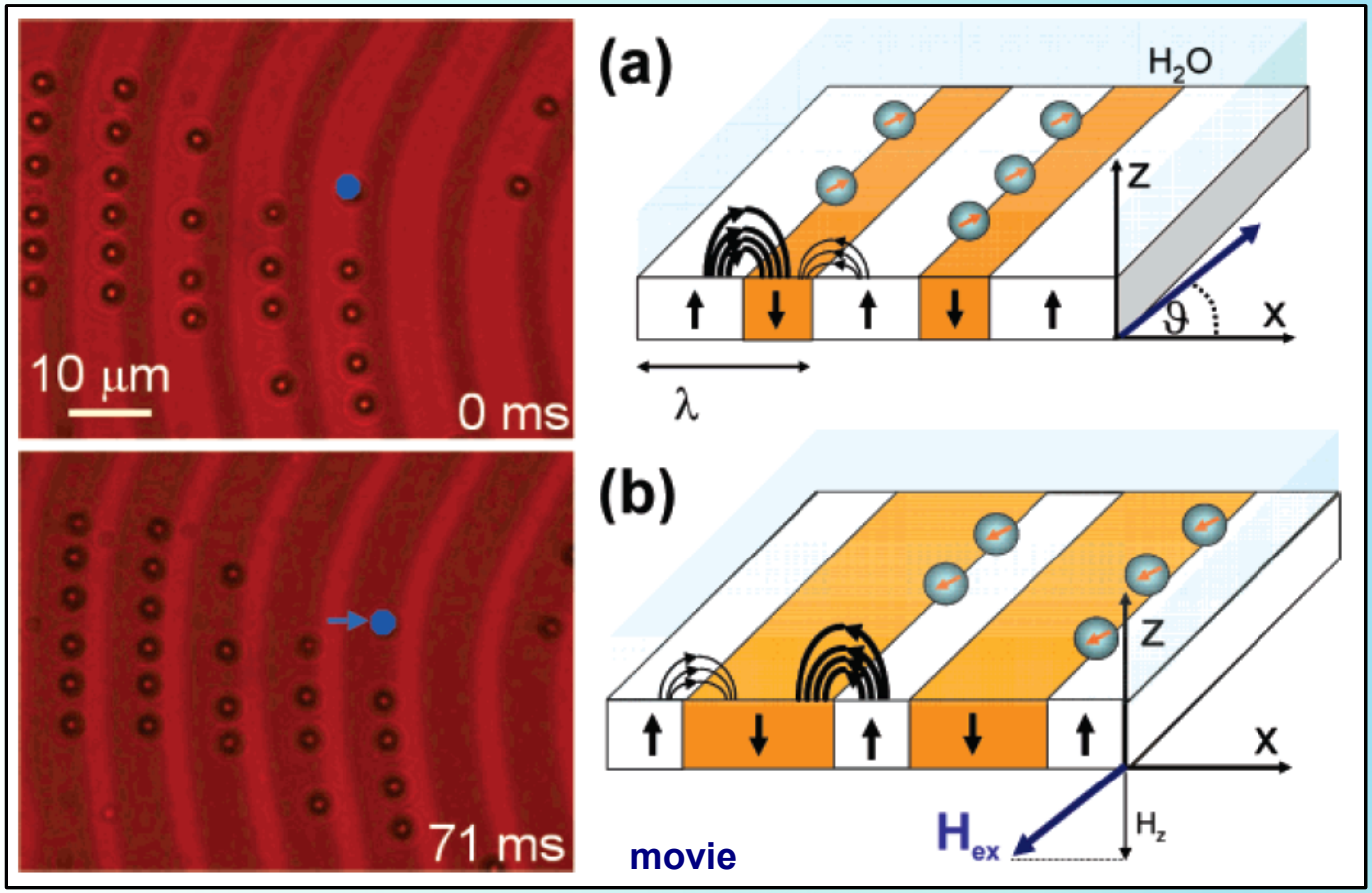

Stripe domain walls stray fields attract magnetic beads placed on the film

λ=10.9 µm

z-component of the external field changes the positions of the domain walls: up and down domains are alternatively wide or narrow

Particles move by **one wavelength in one field cycle**.

$$H_{ext} = 1.3\times10^4[\vec{i}\sin(\omega t)+\vec{k}\sin(\omega t)]\ kA/m$$

$$6\,s^{-1} < \omega < 125\,s^{-1}$$

$$v_p = \frac{\lambda\omega}{2\pi}$$

"Hopping across the domains occurs because the pinning sites alternate between weak and strong during the magnetic modulation of the planar component of the field."

[5] Reprinted with permission from P. Tierno, S. V. Reddy, J. Yuan, T. H. Johansen, and T. M. Fischer, J. Phys. Chem. B , 111, 13479 (2007). Copyright 2007 American Chemical Society.

Colloidal magnetic shift register – oil transport

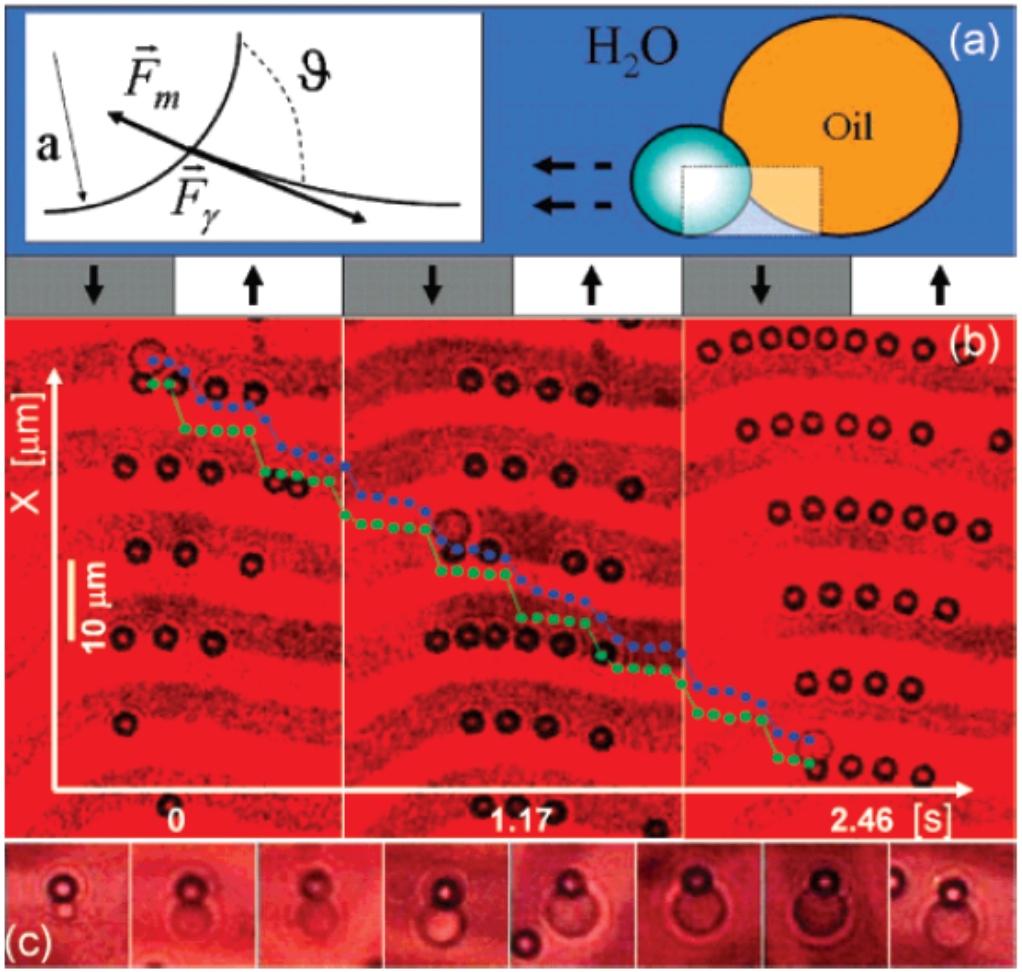

Figure 2. (a) Schematic showing the colloidal particle and oil droplet on the stripe pattern of the garnet film. Inset shows the force diagram at the three-phase (water/oil/particle) contact line. (b) Polarization microscopy images of the particles and oil droplet on the garnet film. The *x* position of one colloidal particle in green and oil droplet in blue is depicted as a function of time. (c) Different images showing differently sized droplets that can be transported by the particles. A corresponding movie of the oil-droplet transport can be found in the Supporting Information.

- **water-oil**: small capillary number ($Ca \approx 10^{-6}$)
  - once attached oil sticks to the magnetic bead
- droplet volume 10^{-19} -10^{-17} liter ($r \approx 4.3$ μm); droplets obtained by sonication
- the magnetic particle size limits the droplet volume
- the stripes period must be adjusted to bead size

speed up to 200 μm/s

[5] Reprinted with permission from P. Tierno, S. V. Reddy, J. Yuan, T. H. Johansen, and T. M. Fischer, J. Phys. Chem. B , 111, 13479 (2007). Copyright 2007 American Chemical Society.

Colloidal magnetic shift register – yeast transport

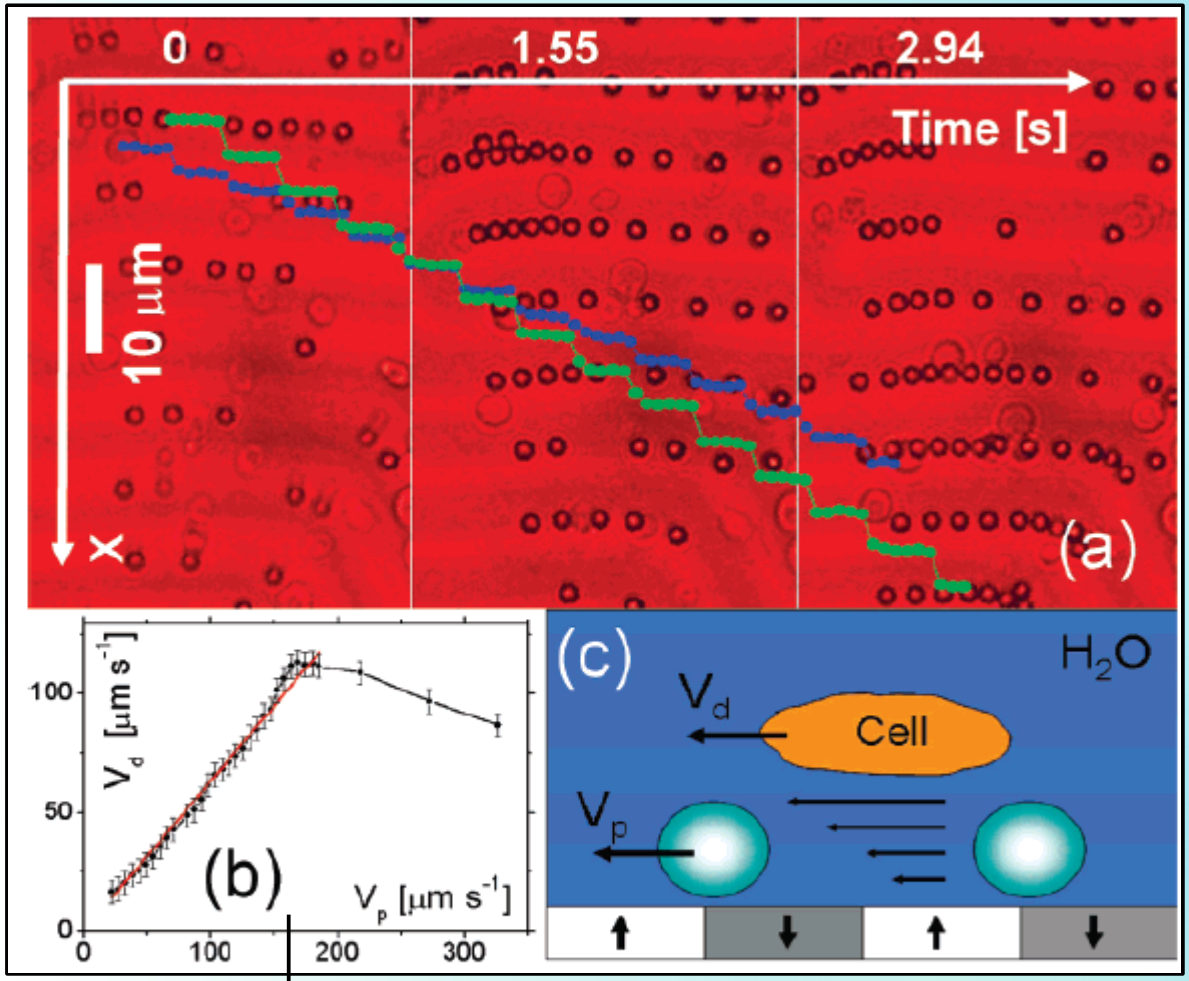

movie

Linear behavior up to 110(?) μm/s

- **secondary flow** generated by the motion of the magnetic particles
- yeast cells are dragged by the secondary flow – noninvasive approach
- both magnetic particles (Dynabeads M-270) and yeast charge negatively in water – no coalescence
- yeast cell levitate above beads

"Variation of the stripe domain wavelength allows the technique to be miniaturized to the nanometer scale which will be useful when dealing with ever smaller amounts of material."

[5] Reprinted with permission from P. Tierno, S. V. Reddy, J. Yuan, T. H. Johansen, and T. M. Fischer, J. Phys. Chem. B , 111, 13479 (2007). Copyright 2007 American Chemical Society.

Mucociliary transport

•In microbiological systems there is a need for a locomotion, nutrients transportation within the organism, and disposal of pollutants (e.g. from respiratory system)

•One common solutions is a **ciliary transport** (cilia- pol. rzęska)

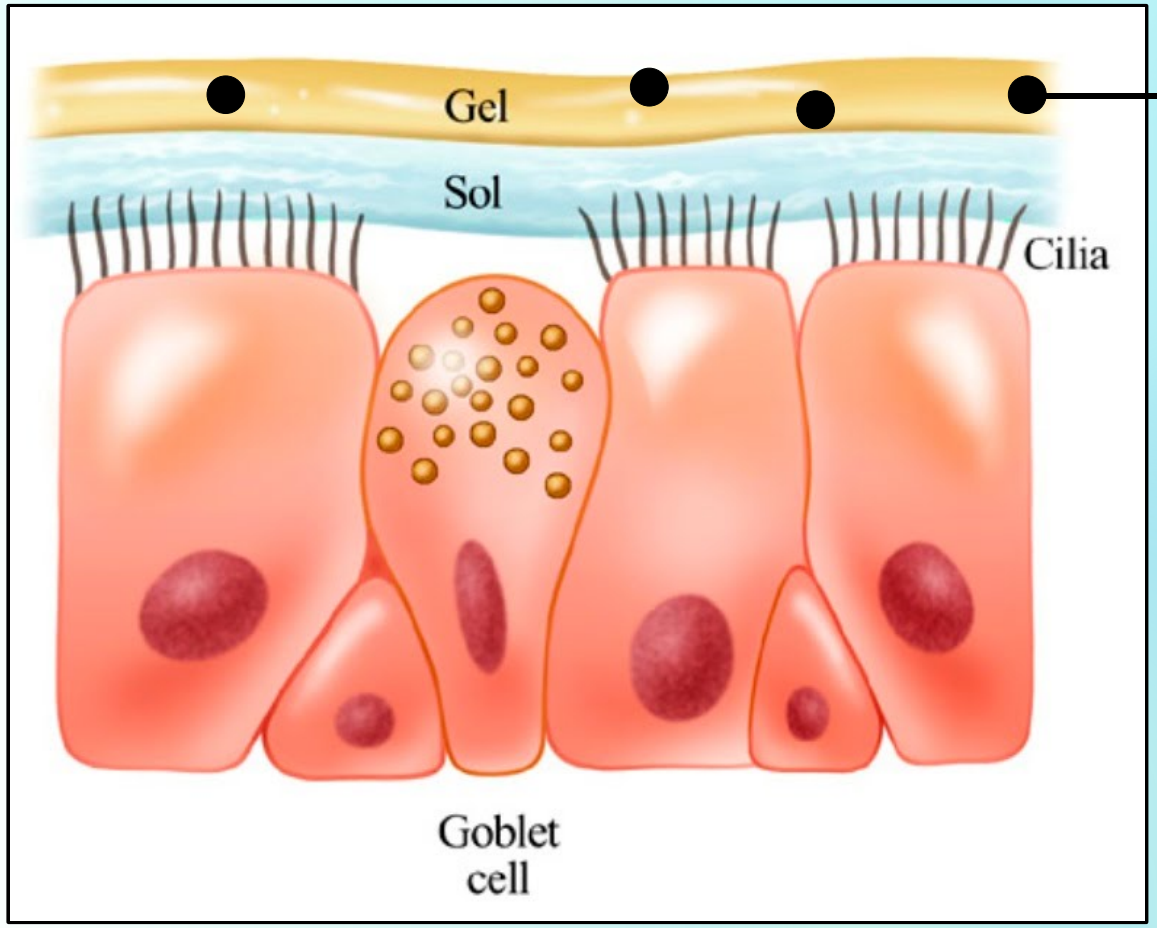

pollutants transported away from the lungs (~10mm/min)

Fig. 2: Schematic representation of how airway mucus is made up of two layers ("sol" and "gel") and how it sits on top of cilia on epithelial cells. The cilia beat is a coordinated way to **move mucus from inside the lungs toward the mouth.**

[16] John V. Fahy, M.D., M.Sc. Asthma [Internet]. Version 11. Knol. 2008 Jul 28

Self-assembled colloidal walkers

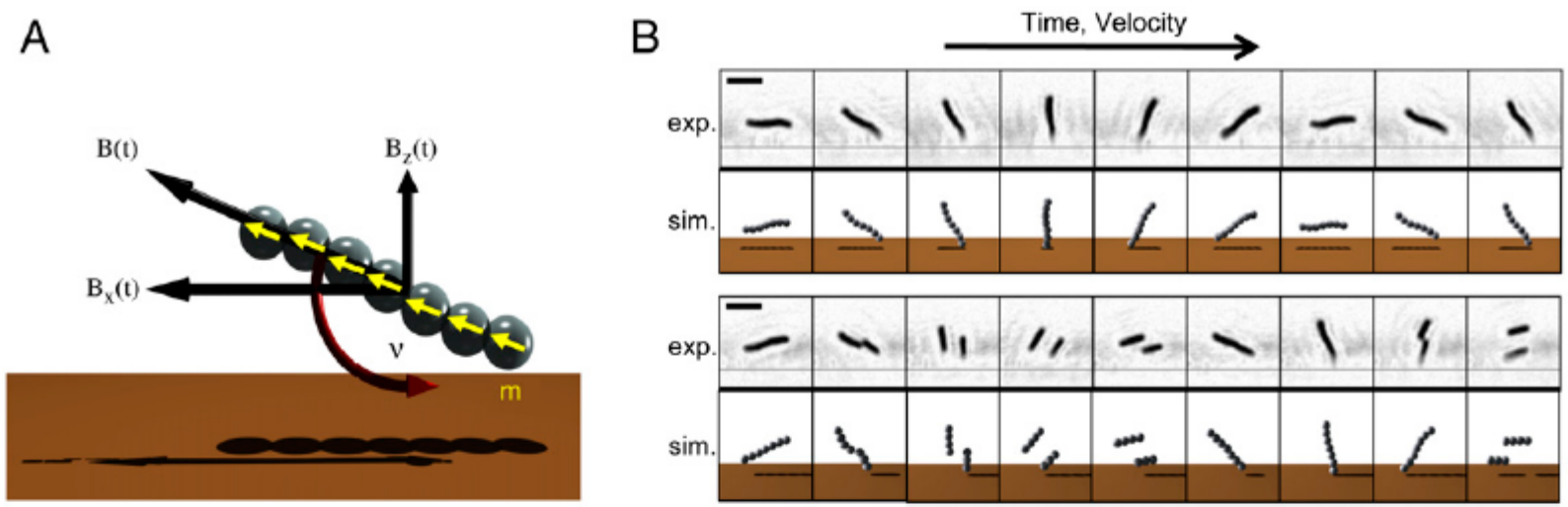

Fig. 1. (*A*) The geometry of "surface walkers". Each chain is composed of superparamagnetic beads that move according to the dynamics of the magnetic field *B* that induces a magnetic moment *m* in each bead. In particular, we focus on rotation along the *x-z* plane at a frequency ν. (*B*) *Top*: The aggregate moves along the surface in both experiment (frames taken 16 ms apart in a 5 Hz rotating field, scale bar is 5 μm) and simulation upon confinement at the surface. *Bottom*: When the field rotation is raised to 7 Hz, the rotors fragment periodically. Notice that the agreement is excellent between both experiments and theory, even in the shape of the fragmented aggregates.

- aqueous solution of 1 μm **superparamagnetic** beads (Dynabeads MyOne™ Carboxylic Acid)
- 10 mT rotating field; frequency: 5-100 Hz
- the chain is driven to assemble upon the application of an external field
- **turning of the field results in disassembly of the aggregates**-possibility to reassemble under different conditions
- gravity keeps the rotors near the surface (other forces applicable: electric, magnetic, etc.)

[7] C. E. Sing, L. Schmid, M. F. Schneider, T. Franke, and A. Alexander-Katz, PNAS, **107**, 535 (2010)

Self-assembled colloidal walkers

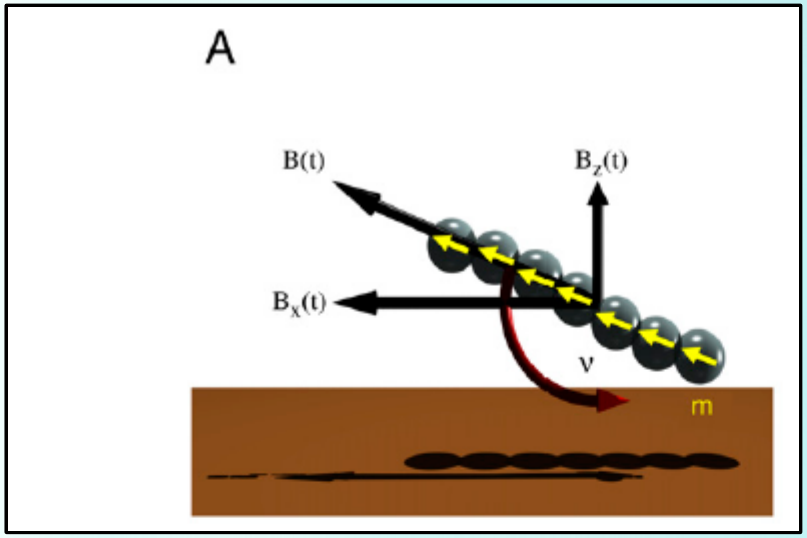

- Upon rotation of the field the chains become μm-sized rotors
- The chain cohesion can be **simply** controlled by the strength of the magnetic field, B
- Field rotates in the plane perpendicular to the substrate surface
- To induce motion **asymmetry is required**

"A simple way to understand this concept is to think of the lower bead (the one closest to the surface) as **a hinge on which the rest of the chain rotates**. This is an oversimplification because friction near the surface remains finite and the bead is allowed to move, but it conveys the essential concept underlying the coupling of rotational motion and translational motion near a surface"

[7] C. E. Sing, L. Schmid, M. F. Schneider, T. Franke, and A. Alexander-Katz, PNAS, **107**, 535 (2010)

Self-assembled colloidal walkers

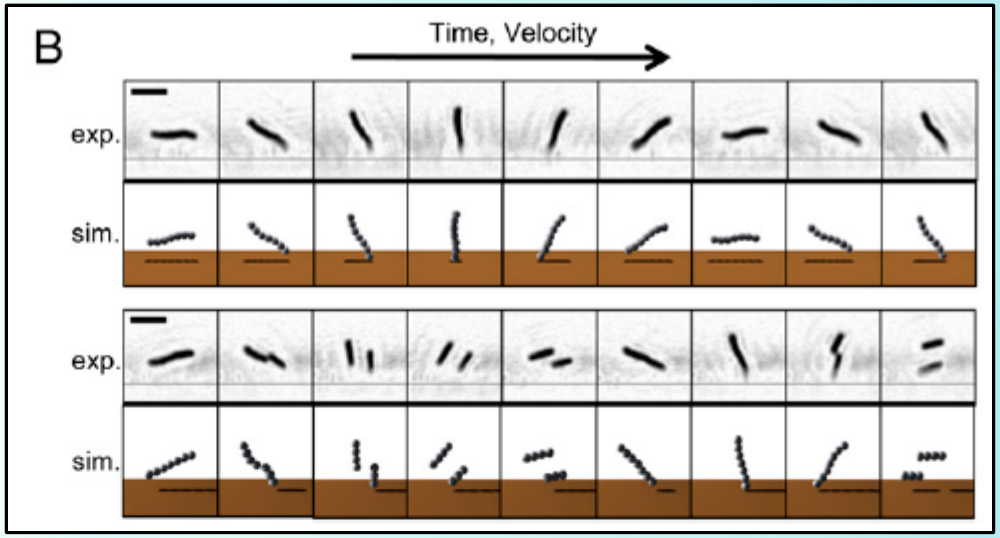

scale bar is 5μm, Δt=16 ms

movie

5 Hz – uniform rotation

7 Hz – **periodic fragmentation**

- Above a critical frequency increased viscous drag forces (maximum magnetic torque remains constant) lead to fragmentation
- There is an excellent agreement between the experiment and hydrodynamic simulations

[7] C. E. Sing, L. Schmid, M. F. Schneider, T. Franke, and A. Alexander-Katz, PNAS, **107**, 535 (2010)

Self-assembled colloidal walkers

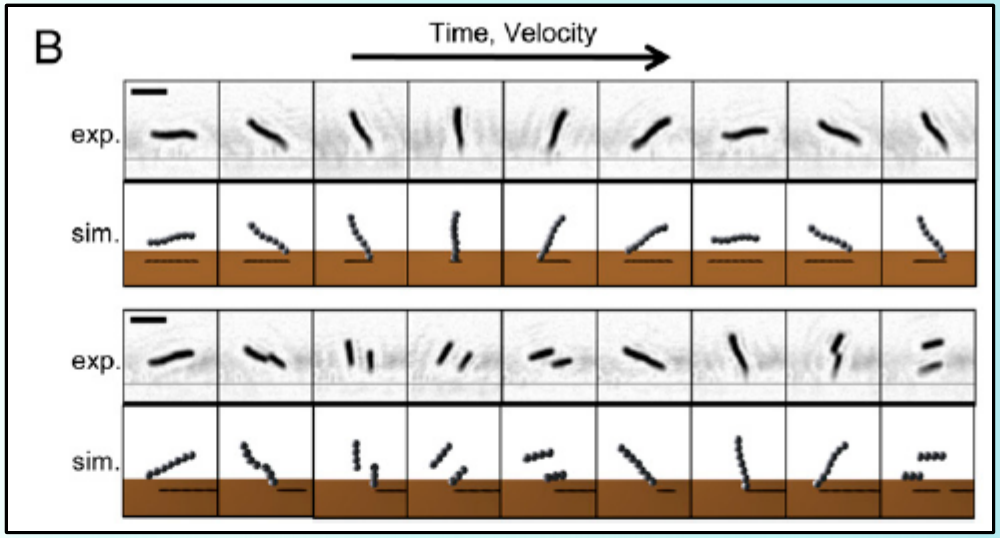

scale bar is 5μm, Δt=16 ms

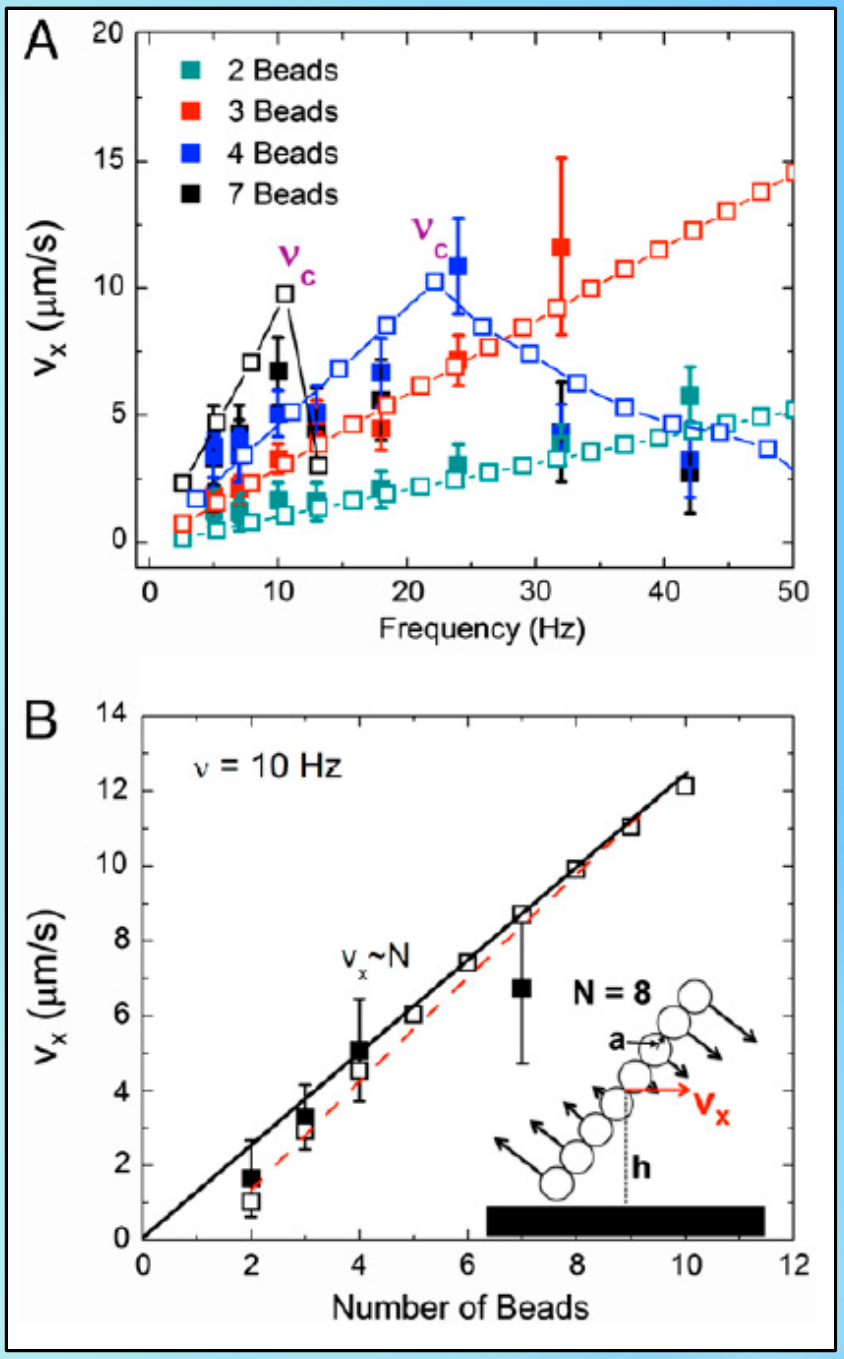

Fig. 2. (*A*) Graph of average translational chain velocity, v_x, versus frequency, ν, as a function of the number of beads. Both experimental (*filled symbols*) and simulation (*open symbols*) results are shown. Lines between simulation points are a guide to the eye. At high ν both the experimental and simulation data suddenly decay to a low-velocity regime due to the onset of chain breakup. (*B*) Graph of the velocity at $\nu = 10$ Hz versus the number of beads in the chain from experiments (*filled symbols*), simulation (*open, black symbols*), and the analytical equation derived in *SI Text* (*red dashed line*). The data quickly approaches the linear regime predicted by using the long-chain limit of the analytical equation (Eq. 1) as demonstrated by the *fit line*. The schematic shown in the inset is a diagram of the geometric variables used in this paper: *a* is the bead radius, *h* is the rotor height (measured from the surface), *N* is the number of beads, and v_x is the translational velocity of the rotor.

[7] C. E. Sing, L. Schmid, M. F. Schneider, T. Franke, and A. Alexander-Katz, PNAS, **107**, 535 (2010)

Self-assembled colloidal walkers – induced flows

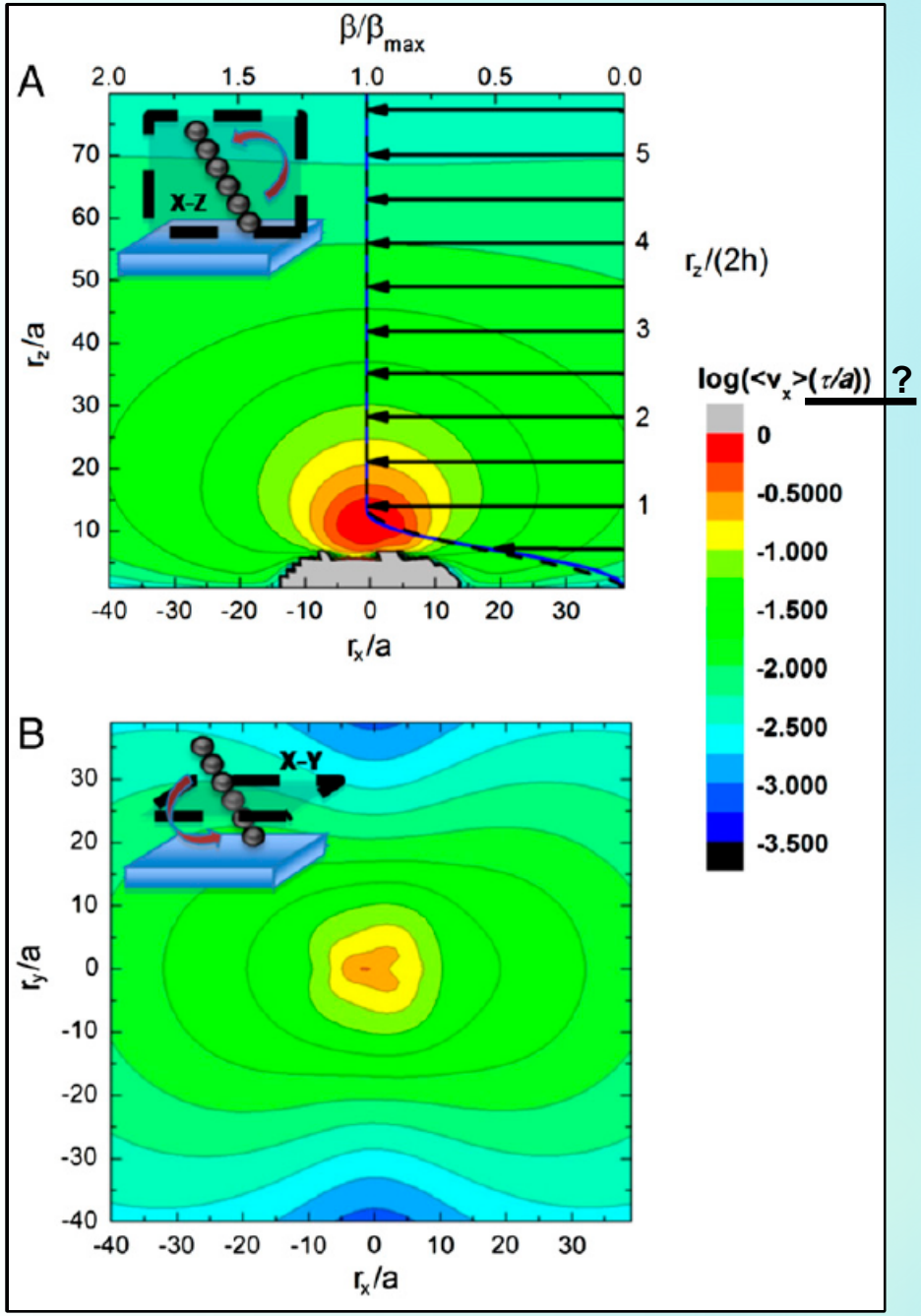

- the velocity profile surrounding a single chain can be obtained from simulations
- there is a considerable **fluid flow in the direction of chain motion**
- flow can be strongly affected by changing the effective (or average) chain length→changing B field strength

Fig. 4. The logarithmic intensity of the x direction of the velocity field immediately surrounding a single seven-bead rotating chain (measured from the chain center of mass), in both the x-z (A) and x-y (B) planes (geometry shown in the cartoon in the *upper left corners*). We also plot on the x-z plane the function β (normalized by β_{max}) as a function of z that is proportional to the mean velocity profile of a collection of rotors as represented in Eq. **5**. Both the simulation (*black dashed*) and analytical (*blue solid*) results for β are shown with the *arrows* representing the direction of the flow. Both profiles are indistinguishable above $z = h$. We note that β tends towards zero near the surface, due to the no-slip condition, and resembles a plug flow profile. The gray area in (A) represents flow that opposes the predominating flow direction and cannot be plotted in the logarithmic scale.

[7] C. E. Sing, L. Schmid, M. F. Schneider, T. Franke, and A. Alexander-Katz, PNAS, **107**, 535 (2010)

Self-assembled colloidal walkers – transport of vesicles

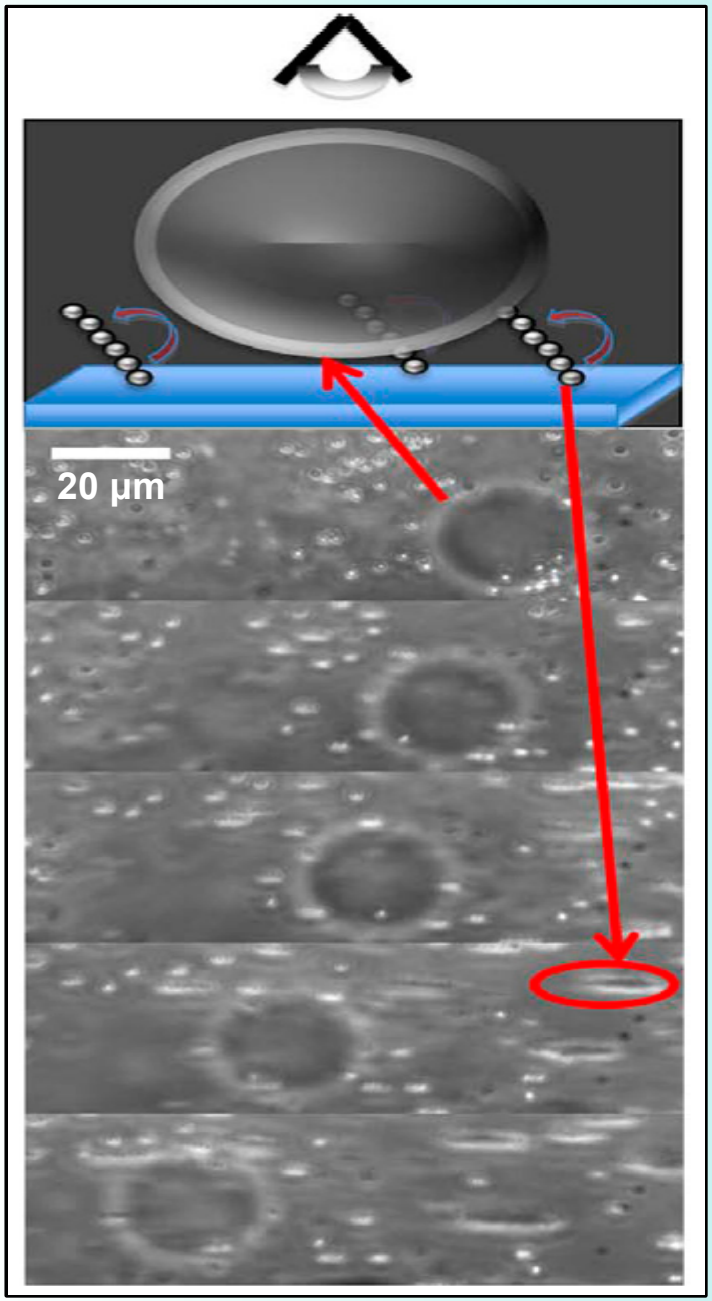

Δt=0.5s

top view

- vesicles prepared by **electroswelling** (electroformation): sucrose inside the vesicle
- beads and vesicles placed in glucose solution – vesicles settle down on the bottom of the chamber
- large vesicles move with **~10 µm/s**
- vesicle motion responds almost immediately to both the initiation and cessation of the field rotation

movie

The method is very cheap and easily adaptable to 2D control (two pairs of Helmholz coils).

Small magnetic field gradients can create gradients in velocity field*.

*Exploiting fragmentation instability

[7] C. E. Sing, L. Schmid, M. F. Schneider, T. Franke, and A. Alexander-Katz, PNAS, **107**, 535 (2010)

Conclusions

•Patterned magnetic media enable a very precise control of the position of the magnetic beads. The method requires a advanced technology for the preparation of substrates. It can be used for the magnetic separation

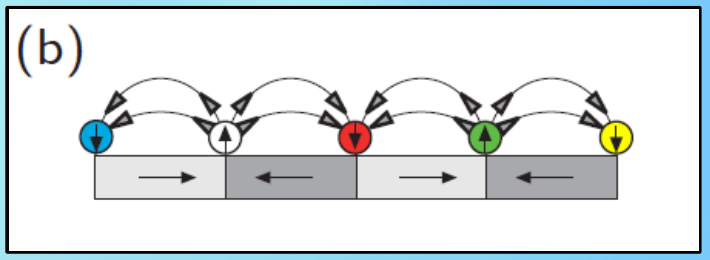

Conclusions

•Patterned magnetic media enable a very precise control of the position of the magnetic beads. The method requires a advanced technology for the preparation of substrates. It can be used for the magnetic separation

•Magnetic shift register on garnets with stripe domains is precise and can be scaled down to nanometer scale by changing the spatial period of the stripes

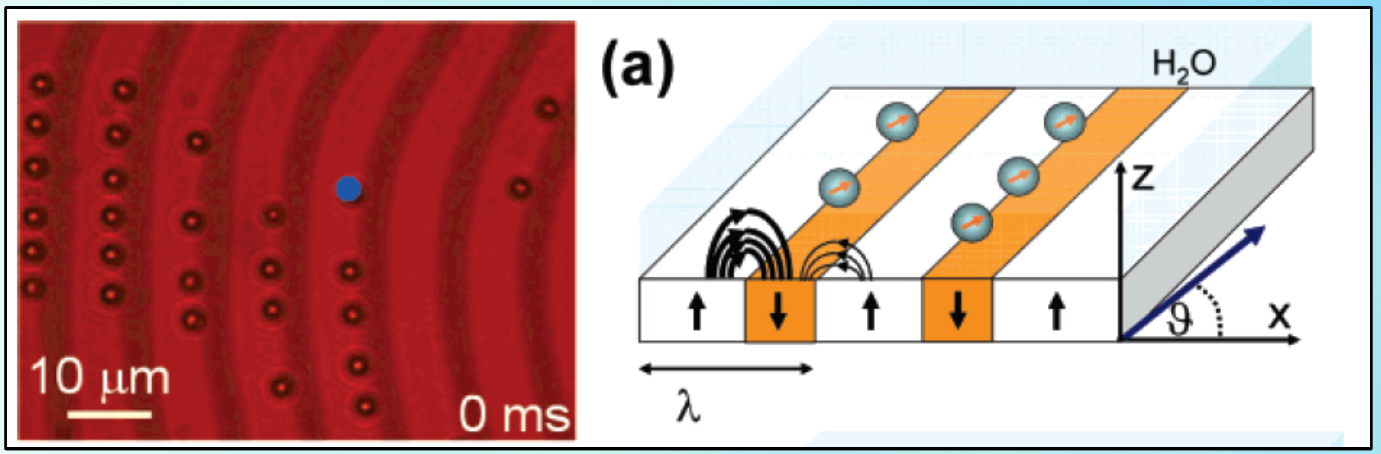

Conclusions

•Patterned magne ontrol of the position of the magnetic beads. T nology for the preparation of substrates. It can

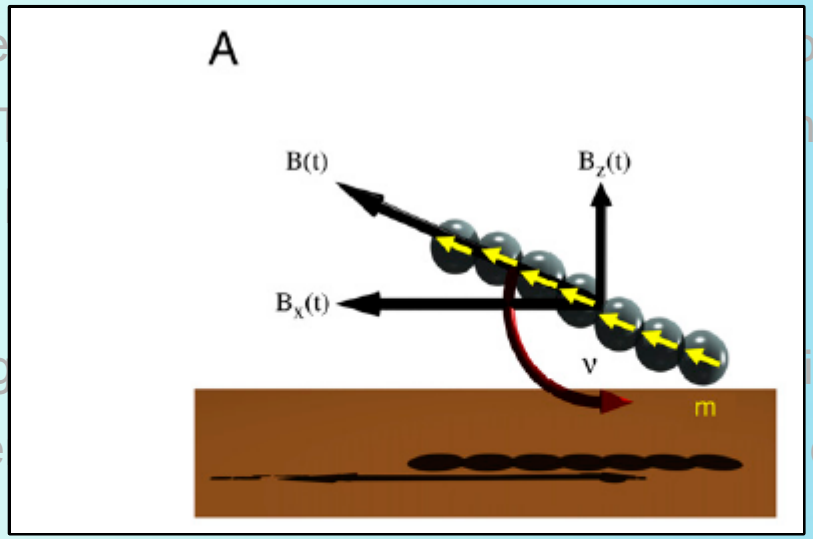

•Magnetic shift reg is precise and can be scaled down to nanomete of the stripes

•Colloidal walkers provide very simple and cheap means of transport of large particles without the need for binding to magnetic beads. The method is not applicable to magnetic separation

Conclusions

•Patterned magnetic media enable a very precise control of the position of the magnetic beads. The method requires a advanced technology for the preparation of substrates. It can be used for the magnetic separation

•Magnetic shift register on garnets with stripe domains is precise and can be scaled down to nanometer scale by changing the spatial period of the stripes

•Colloidal walkers provide very simple and cheap means of transport of large particles without the need for binding to magnetic beads. The method is not applicable to magnetic separation

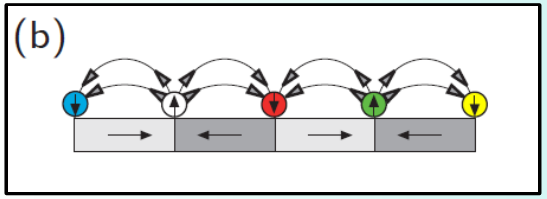

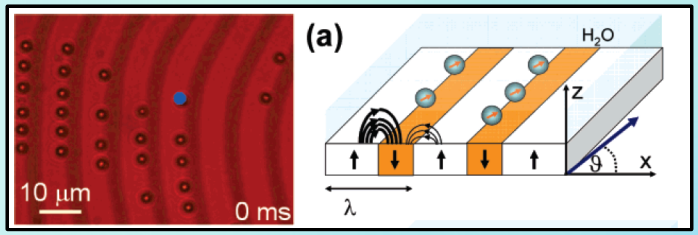

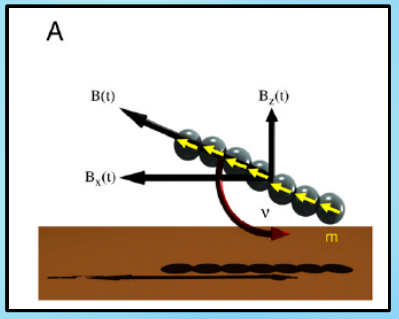

Acknowledgements

Following software was used in preparation of this document:

- OpenOffice.org 3.0.0 (www.openoffice.org)
- Inkscape 0.46 (www.inkscape.org)
- Sage (www.sagemath.org)